Parametric Estimation of Stochastic Fading Channels and Their Role in Adaptive Radios

Joseph D. Gaeddert

Thesis submitted to the Faculty of the
Virginia Polytechnic Institute and State University
in partial fulfillment of the requirements for the degree of

Master of Science
in
Electrical Engineering

Dr. A. Annamalai, Chair
Dr. J. H. Reed
Dr. W. H. Tranter

February 7, 2005
Blacksburg, Virginia

Keywords: Wireless, Adaptive Radio, Channel Estimation, Nakagmi-m, Weibull, Rice-K, Adaptive Modulation, Log-normal shadowing, BER Approximations

Parametric Estimation of Stochastic Fading Channels and Their Role in Adaptive Radios

Joseph D. Gaeddert

ABSTRACT

The detrimental effects rapid power fluctuation has on wireless narrowband communication channels has long been a concern of the mobile radio community as appropriate channel models seek to gauge link quality. Furthermore, advances in signal processing capabilities and the desire for spectrally efficient and low power radio systems have rekindled the interest for adaptive transmission schemes, hence some method of quickly probing the link quality and/or predicting channel conditions is required. Mathematical distributions for modeling the channel profile seek to estimate fading parameters from a finite number of discrete time samples of signal amplitude. While the statistical inference of such estimators has proven to be robust to rapidly shifting channel conditions, the benefits are quickly realized at the expense of processing complexity. Furthermore, computations of the best-known estimation techniques are often iterative, tedious, and complex.

This thesis takes a renewed look at estimating fading parameters for the Nakagami-m, Rice-K, and Weibull distributions, specifically by showing that the need to solve transcendental equations in the estimators can be circumvented through use of polynomial approximation in the least-squared error sense or via asymptotic series expansion which often lead to closed-form and simplified expressions. These new estimators are compared to existing ones, the performances of which are comparable while preserving a lower computational complexity. In addition, the thesis also investigates the impact knowledge of the fading profile has on systems employing adaptive switching modulation schemes by characterizing performance in terms of average bit error rates (BER) and spectral efficiency. A channel undergoing Rice-K fading on top of log-normal shadowing is simulated by correlating samples of received signal amplitude according to the user's doppler speed, carrier frequency, etc. The channel's throughput and BER performances are analyzed using the above estimation techniques and compared to non-estimation assumptions. Further discussion on narrowband fading parameter estimation and its applicability to wireless communication channels is provided.

This work received support from the Mobile and Portable Radio Research Group (MPRG) at Virginia Tech.

Acknowledgments

I would like to thank Dr. Annamalai and the precious faculty, staff, and students at MPRG whose endless support made this work possible.

List of Abbreviations

ABER	Approximate bit error rate
AGME	Approximate generalized moment estimator
AMLE	Approximate maximum-likelihood estimator
AoA	Angle of arrival
AWGN	Additive white Gaussian noise
BER	Bit error rate
CDF	Cumulative distribution function
CRLB	Cramér-Rao lower bound
GME	Generalized moment estimator
IGME	Iterative generalized moment estimator
IMLE	Iterative maximum-likelihood estimator
i.i.d.	Independent and identically distributed
LLF	Log-likelihood function
LoS	Line of sight
MC	Modified Cran estimator (Weibull)
MGF	Moment generating Function, $\Phi(s)$
MGME	Modified Generalized moment estimator
MLE	Maximum-likelihood estimator
mMGF	Marginal moment generating function, $\phi(s, x)$
PDF	Probability density function
PE	Percentile estimator
PSD	Power spectral density
PSK	Phase shift keying
QAM	Quadrature amplitude modulation
QoS	Quality of Service
RMSE	Root mean-square error
RV	Random variable
SER	Symbol error rate
SNR	Signal to noise ratio

Contents

List of Figures

List of Tables

Chapter 1

Introduction

1.1 Motivation

With the growing popularity of channel aware, adaptive, and cognitive radios and the detrimental effects rapid power fluctuations have on wireless communications come the need for quickly gauging link quality. Furthermore, advances in signal processing capabilities and the desire for spectrally efficient and low power radio systems have rekindled the interest for adaptive transmission schemes, hence some method of quickly probing the link quality and/or predicting channel conditions is required.

1.2 "Blind" channel state estimation

Recently a number of papers have developed methods of estimating fading parameters (e.g. mean power, signal threshold, and fading severity) from a finite number of independent and identically distributed (i.i.d.) samples, robust to quickly changing channel conditions. The optimum choice for parameter estimation over a finite sample set is the minimum variance unbiased estimator (MVUE) as it provides the most powerful procedure for testing unknown parameters, however due to processing constraints practical use of MVUEs is limited. Similarly, the best linear unbiased estimator (BLUE) is not used in practice due to the processing requirements to invert variance-covariance matrices, especially with large sample sizes.

Indirect methods for gauging link quality, often realized in packet error rates, have been proposed in [1], however extended transmission times are required to gather a sufficient number of packets to appropriately determine quality of service, and thus cannot adequately match to quickly changing channel conditions. Direct methods baed on statistical inference of received instantaneous power require less time over which to estimate the fading profile and thus are adaptive to fast fluctuations in the channel's environment. Additionally because

such methods are based on received signal strength alone, no *apriori* knowledge of the channel or data is needed, thus reducing overhead in pilot symbol assisted modulation systems.

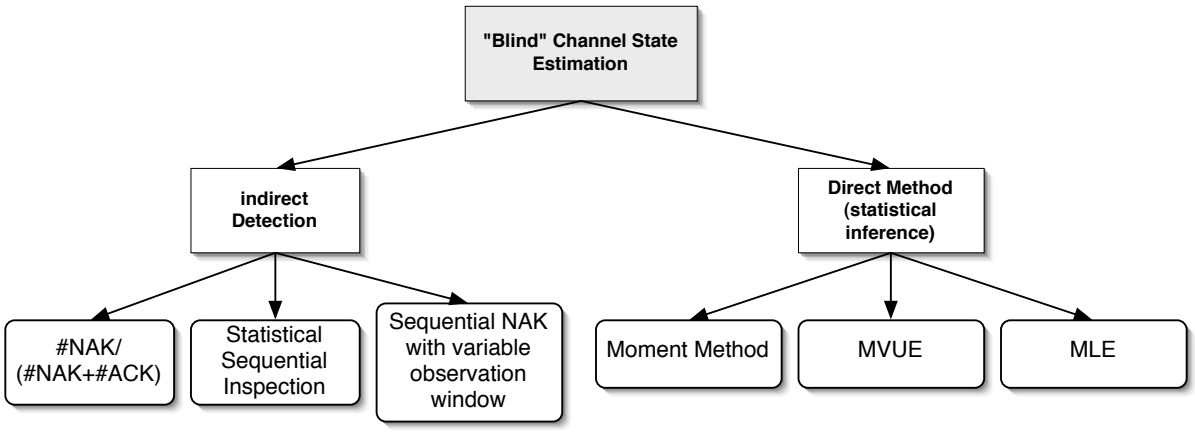

Figure 1.1: Channel estimation techniques

Mathematical distributions for modeling the channel profile seek to estimate fading parameters from a finite number of discrete time samples of signal amplitude. While the statistical inference of such estimators has proven to be robust to rapidly shifting channel conditions, the benefits are quickly realized at the expense of processing complexity. Furthermore, computations of the best-known estimation techniques are often iterative, tedious, and complex.

1.3 Contributions

The contributions channel estimators have on modern communications systems is most apparent in adaptive and cognitive radios. Besides developing advances mentioned above in receiver diversity combining schemes, fading channel parameter estimation can be applied to optimal power allocation in transmit diversity systems, and hybrid antenna arrays with adaptive switching between different operational modes. Furthermore, it is also of interest to consider the benefits of adaptive radio transmissions from an information theory standpoint. The results of fundamental limits to wireline communications channels [2] have recently been extended to wireless systems, including channels with diversity. Wireless systems, however, are designed for multi-user support, thus dividing the capacity between the users. This naturally motivates the work on channel sensing to extend towards technologies such as adaptive modulation, opportunistic scheduling, and routing protocols, where knowledge of average and outage capacities are important for developing system design guidelines.

This work takes a renewed look at estimating statistical fading parameters for the Nakagami-m, Rice-K, and Weibull distributions based on statistical inference of received signal strength

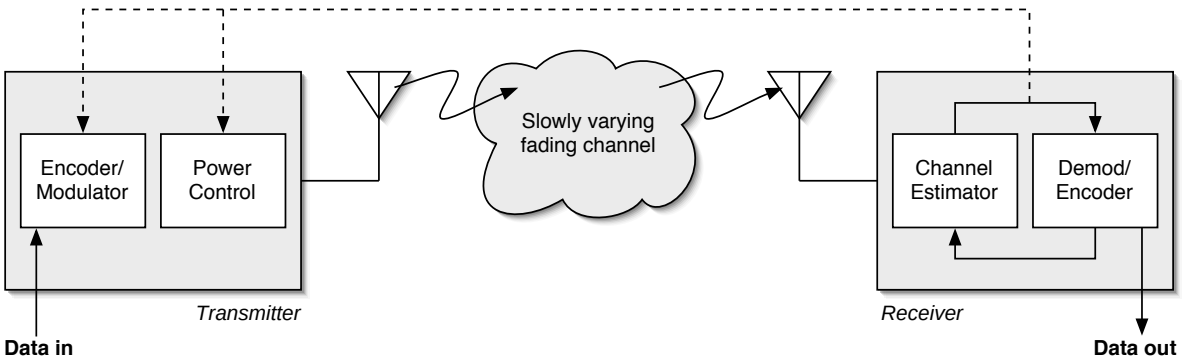

Figure 1.2: Adaptive radio

alone, specifically by demonstrating the need to solve transcendental equations in the estimators can be circumvented through polynomial approximations or by asymptotic series expansions. The results of such techniques are simplified expressions for estimators which can often be written in closed form, thus eliminating the need for iterative techniques or complex matrix inversion algorithms while preserving a low computational budget. Furthermore a statistical commparison of the new channel estimators to existing solutions is presented, the results of which suggest that estimators based on approximations can even outperform exact solutions, primarily due to being able to choose functions which better describe the data.

In addition, the work also investigates the impact accurate knowledge of the channel has on systems employing adaptive modulation-switching schemes by characterizing its performance under the mathematical fading model in additive white Gaussian noise channels. A unified expression for adaptive bit error rates and average spectral efficiencies are developed for the systems, and performance is simulated by generating random fading envelopes and analyzed against systems that make only basic assumptions about the channel's fading characteristics.

Chapter 2

Nakagami-m Parameter Estimation

2.1 Introduction

Nakagami-m distribution is a versatile stochastic model for modeling radio links [3] and has often been regarded as the best distribution to model land mobile propagation due to its ability to describe fading situations worse than Rayleigh, including one-sided Gaussian [4]. Empirical evidence regarding the efficacy the Nakagami-m distribution has on fading profiles been presented in [5, 6]. Thus statistical inference of the Nakagami-m fading parameters are of interest in the design of adaptive radios such as optimized transmit diversity modes [7, 8] and adaptive modulation schemes [9]. Estimators for the Nakagami-m fading parameter m using maximum-likelihood, integer moments, and real moments techniques have been proposed in [10, 11, 12, 13] and references therein.

This chapter takes a renewed look at the estimation of the m parameter. Specifically, we show that the need to solve the transcendental equations on which the estimators are based can be circumvented through use of a quadratic polynomial approximation in the least-squared error sense or via an asymptotic series approximation, that lead to closed-form expressions for estimating m from the sample moments. Several methods for estimating the Nakagami-m fading parameters are proposed, including those based on moments as well as maximum-likelihood. Also included is a proof that exponential variable transformation on sample data does not improve maximum-likelihood estimators as it can for moment-based estimators.

2.2 Generalized Moment-Based Estimators

As discussed in Section 1.2, estimators based on moments provide an effective, simple, and often closed form estimation for stochastic channel parameters without the need to iteratively

solve complex functions or invert complex matrices. Many moment-based estimators, however, rely on higher-order moments in order to solve for fading parameters in closed-form which tend to differ from theoretical moments due to being susceptible to ouliers. However, resolving equations relying on lower order moments requires inverting transcendental equations. Numerical inversion methods are often inappropriate in wireless systems as they require unavailable computational bandwidths. In order to circumvent these issues, this section describes several methods to developing closed-form estimates through polynomial approximations.

2.2.1 Moment Estimator Forms

Given N independent and identically distributed (i.i.d) samples $\{r_1, r_2, \ldots, r_N\}$ of signal amplitude drawn from a Nakagami-m population [14],

$$f_R(r; m, \Omega) = \frac{2}{\Gamma(m)} \left(\frac{m}{\Omega}\right)^m r^{2m-1} e^{-mr^2/\Omega} \tag{2.1}$$

with fading severity index m and average power $\Omega = E\{R^2\}$ ($\Gamma(x)$ is the Gamma function, see Appendix A), moment-based estimators seek to estimate parameter m using only the sample moments of the random fading amplitude R, defined as

$$\hat{\mu}_k = (1/N) \sum_{i=1}^{N} (r_i)^k \tag{2.2}$$

By matching the sample moments to theoretical moments, the m-parameter can be uniquely determined. The k^{th} moment of the random fading amplitude R can be derived without considerable difficulty as

$$\mu_k = E\left\{R^k\right\} = \frac{\Gamma\left(m + \frac{k}{2}\right)}{\Gamma\left(m\right)} \left(\frac{\Omega}{m}\right)^{\frac{k}{2}} \tag{2.3}$$

In effort to develop estimators for the m parameter independent of Ω, ratios of moments are used to eliminate the Ω term in (2.3). In [12], Cheng and Beaulieu elegantly showed that better moment-based estimators can be found by admitting the use of noninteger moments. Hence using variable transformation $Y = R^{1/p}$ where $\mathrm{Re}\{p\} > 0$, the k^{th} moment of Y is given by [12, Eq. (6)]

$$\mu_{k/p} = E\left\{Y^k\right\} = E\left\{R^{k/p}\right\} = \frac{\Gamma\left(m + \frac{k}{2p}\right)}{\Gamma\left(m\right)} \left(\frac{\Omega}{m}\right)^{\frac{k}{2p}} \tag{2.4}$$

Form 1

A family of m parameter estimators can be developed by taking the ratio of any two moments of Y and solving for m, viz.,

$$\Delta_{a,b,p} = \frac{\hat{\mu}_{a/p}}{(\hat{\mu}_2)^{\frac{a-b}{2p}}\hat{\mu}_{b/p}} = \frac{\Gamma\left(\hat{m}+\frac{a}{2p}\right)}{\Gamma\left(\hat{m}+\frac{b}{2p}\right)\hat{m}^{\frac{a-b}{2p}}} \tag{2.5}$$

where $a \neq b$ are arbitrary nonnegative integers. In general, such a procedure involves solving a transcendental equation and does not lead to a closed-form expression for the estimator. For this reason, [12] and [10] have resorted to higher order sample moments to derive $\hat{m}$ in closed form. However, recognizing that higher order sample moments deviate from the theoretical moments, consequently in the process of modeling finite number of samples (empirical data) the optimum choice for (a, b) is $(1, 0)$ (i.e., setting $k = 1$ in (2.4)).

Form 2

It is obvious that the ratio $(\mu_{\alpha/p})^\beta/(\mu_{\beta/p})^\alpha$ for $\alpha \neq \beta$ also leads to a family of real moment estimators for the fading parameter m because it depends only on m and is independent of Ω. The natural choice for (α, β) is $(1, 2)$ regardless of the choice of p since this selection involves the lowest order moments, viz.,

$$\Delta_{GME} = \frac{\left(\mu_{1/p}\right)^2}{\mu_{2/p}} = \frac{\left[\Gamma\left(m+\frac{1}{2p}\right)\right]^2}{\Gamma(m)\,\Gamma\left(m+\frac{1}{p}\right)} \tag{2.6}$$

For a specific p, we can expect that the variance of this estimator to be smaller than any other combinations of α and β. However, we again face a dilemma in solving the above transcendental equation for m in closed form. For this reason, previous studies [10] and [12] have resorted to higher order moments instead, at the expense of a slight degradation in the performance of their estimators. Notice that $\Delta_{1,0,p} = \Delta_{GME}$ when $p = 1$. Iterative solutions to (2.6) for various values of p are denoted as IGME.

2.2.2 Approximate Generalized Moment Estimators

Neither of the two forms presented in Section 2.2.1 leads to a closed-form solution to m. Iterative methods give the best solution and provide a benchmark for comparing approximate estimators, however they can be cumbersome, slow, and inappropriate for practical mobile applications. Approximate solutions, however, are efficient can provide simple, closed-form solutions where otherwise none is avilable. Exploiting the nature of the ratio of two Gamma

functions, a closed-form, but an approximate estimator for $\hat{m}$ may be obtained by approximating the right side of (2.5) using [15, pp. 11] as

$$\Delta_{a,b,p} = \sum_{k=1}^{Q-1} (-1)^k \frac{\left(\frac{b-a}{2p}\right)_k}{k! m^k} B_k^{\left(\frac{a-b}{2p}+1\right)} \left(\frac{a}{2p}\right) + O\left(m^{-Q}\right) \tag{2.7}$$

where $(a)_k$ denotes the Pochhammer symbol and $B_k^{(x)}(y)$ is the generalized Bernoulli polynomial [15, pp. 505]. If $\frac{a-b}{2p} = (Q-1)$ is a positive integer, then (2.7) is exact (i.e., the $O(m^{-Q})$ remainder term can be ignored). This property will be exploited in Section 2.2.3 in order to derive a family of generalized moment-based estimators for the m parameter.

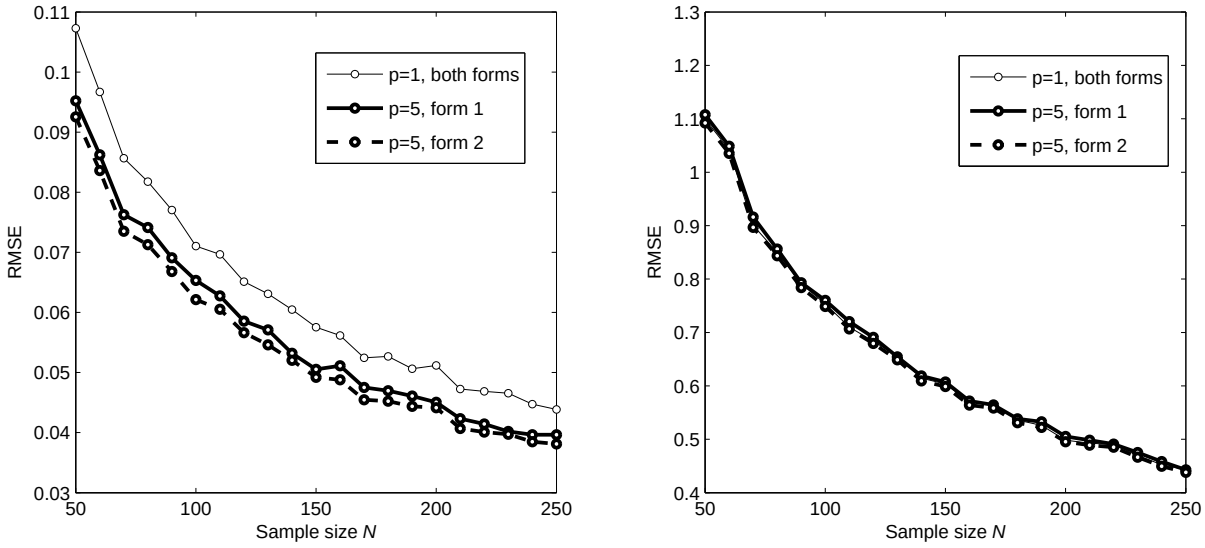

(a) $m = 0.5$ (b) $m = 5$

Figure 2.1: Root mean-square error for iterative solutions to form 1 (2.5) with $a = 1$ and $b = 0$ and form 2 (2.6) versus sample size N averaged over 2,500 independent trials.

Truncating the series (2.7) to the first three terms (second-order approximation), gives

$$\Delta_{a,b,p} \approx 1 + \frac{(a-b)(a+b-2p)}{8p^2\hat{m}} + \frac{(a-b)(a-b-2p)}{384p^4\hat{m}^2} \times \left[3(a+b-2p)^2 - (a-b+2p)2p\right] \tag{2.8}$$

Recognizing that (2.8) is obtained from an asymptotic series expansion, a slightly more general estimator may be devised by writing (2.8) in the form

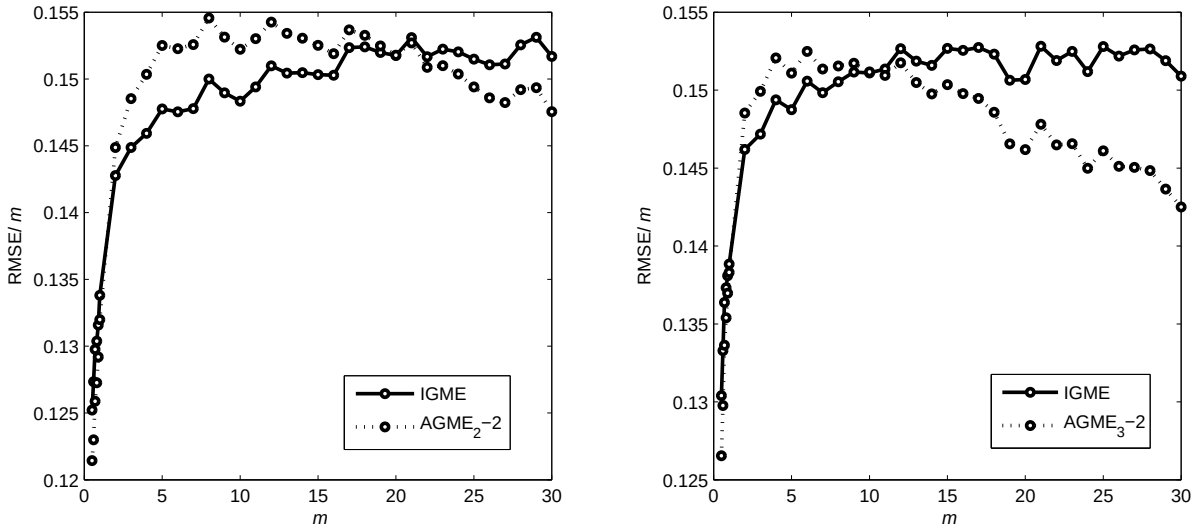

(a) Form 1, (2.5)

(b) Form 2, (2.6)

Figure 2.2: Normalized root mean-square error for iterative estimators and their respective approximating functions averaged over 5,000 trials and plotted versus m for a sample size $N = 100$.

$$\Delta_{a,b,p} \approx c_0 + \frac{c_1}{m} + \frac{c_2}{m^2} \tag{2.9}$$

where the coefficients c_0, c_1, and c_2 can be obtained either from substituting a, b, and p into (2.8) or by polynomial curve-fitting (2.9) to the right side of (2.5). Note that the right side of (2.8) is a monotonically increasing function in the interval $m \in (0.5,\infty)$, and the ratio varies from 0 to 1. Letting $a = 1$ and $b = 0$ in (2.9) and solving the above equation for $\hat{m}$, a new family of approximate moment estimators for $\hat{m}$ can be obtained as

$$\hat{m} = \frac{-c_1 - \sqrt{c_1^2 - 4(c_0 - \Delta_{1,0,p})c_2}}{2(c_0 - \Delta_{1,0,p})} \tag{2.10}$$

where $\Delta_{1,0,p} = \frac{\hat{\mu}_{1/p}}{(\hat{\mu}_2)^{1/2p}}$ and the coefficients c_0, c_1, and c_2 are summarized in Table 2.1 (denoted with subscript 1) for several values of p.

The performance of (2.10) can be further improved by optimizing the coefficients c_0, c_1, and c_2 for the practical range of $0.5 \leq m \leq 30$ using Quasi-Newton method (i.e., curve fitting the right side of (2.5) to (2.9) in the least squared error sense). These results are also summarized in Table 2.1 (subscript 2) for several values of p. It should be evident that the computational budget for the new estimators are lower compared to [12, Eqs. (4) and (9)] since the latter

Table 2.1: Optimized coefficients for integer and generalized moment-based Nakagami m-parameter estimators

		c_0	c_1	c_2
AGME$_1$-2	$p=1$	1	-1.2500E-1	7.8125E-3
	$p=5$	1	-4.5000E-2	-4.9875E-3
	$p=10$	1	-2.3750E-2	-3.2805E-3
AGME$_2$-2	$p=1$	1.0000E+0	-1.2623E-1	1.2565E-2
	$p=5$	1.0000E+0	-4.6194E-2	-2.1243E-3
	$p=10$	1.0000E+0	-2.4298E-2	-2.0365E-3
AGME$_3$-1	$p=1$	9.9709E-1	-2.0821E-1	
	$p=5$	1.0003E+0	-1.4996E-2	
	$p=10$	1.0001E+0	-4.1072E-3	
	$p=20$	1.0000E+0	-1.0774E-3	
AGME$_3$-2	$p=1$	9.9997E-1	-2.4986E-1	3.4793E-2
	$p=5$	1.0000E+0	-1.0128E-2	-4.0668E-3
	$p=10$	1.0000E+0	-2.4124E-3	-1.4159E-3
	$p=20$	1.0000E+0	-5.7870E-4	-4.1607E-4

require evaluation of three sample moments for estimating $\hat{m}$ (which is undesireable as N gets larger).

Exploiting the same asymptotic approximation for a ratio of two Gamma functions [15, pp. 11], the right side of (2.6) can be expanded (after considerable algebraic manipulation) as

$$\Delta_{GME} = 1 - \frac{1}{4p^2m} - \frac{4p^2-4p-1}{32p^4m^2} + \ldots \tag{2.11}$$

which is of the same form as (2.9) and thus (2.10) can be used as an approximate generalized moment estimator for m, with the substitution $\Delta_{GME} = (\hat{\mu}_{1/p})^2/\hat{\mu}_{2/p}$ for $\Delta_{1,0,p}$. The optimized coefficients are summarized in Table 2.1 (subscript 3) for several values of p.

Considering only a linear polynomial approximation in (2.5) (i.e., $c_2 = 0$),gives

$$\hat{m} = \frac{c_1}{\Delta_{GME} - c_0} \tag{2.12}$$

Although the moment-based estimator performance may be improved slightly with a higher order polynomial approximation (e.g., cubic or quartic), inverting such polynomials becomes increasingly difficult, the effectiveness of will be left to maximum-likelihood estimation in section 2.3. Moreover, numerical results reveal that (2.10) already exhibits very good performance, and therefore $\hat{m}$ obtained from cubic or quartic polynomial inversion will yield only marginal improvement. Nevertheless, (2.10) yields considerably better performance over (2.12).

Notice that the use of the fractional (real) moment estimator derived in [12] will give rise to the computational complexity over (2.10) since in our case only two (instead of three) sample moments are needed. However, the coefficients c_0, c_1 and c_2 must be optimized uniquely for each value of p (which can be performed off-line). Alternatively, we may use the coefficients from the asymptotic series in (2.8) and (2.11). The statistical properties of the new moment-based estimators are examined using Monte Carlo simulations in Figures 2.5, 2.6, 2.7, 2.8, 2.9, and 2.10.

2.2.3 Exact Generalized Moment-Based Estimators

Using the same framework in Section 2.2.2, certain circumstances provide exact moment-based estimators for the m parameter. In fact, previously discovered exact moment-based estimators [12, Eq. (4)], [12, Eq. (9)], and [12, Eq. (5)] can be obtained from (2.7). Setting $\frac{a-b}{2p} = 1$ in (2.7), yields

$$\Delta_{2p+b,b,p} = 1 + \frac{b}{2p\hat{m}} \tag{2.13}$$

because the series terminates (all other higher order terms reduce to zero). Hence, an exact GME for $\hat{m}$ is given by

$$\hat{m} = \frac{\delta\hat{\mu}_2\hat{\mu}_\delta}{2(\hat{\mu}_{2+\delta} - \hat{\mu}_2\hat{\mu}_\delta)} \tag{2.14}$$

where $\delta = b/p$. The expression is slightly more general than [12, Eq. (9)] because b is not restricted to 1.

Such exact generalized moment-based estimators will be hereafter referred to as EGME$_\delta$. Although these estimators are exact, they do not necessarily prove to be better than approximate GMEs. This is likely due to their dependence upon higher-order moments. Figure 2.2.3 demonstrates that as δ approaches 0, the performance of EGME$_\delta$ is similar to IGME ($p = 1$). Notice that as δ approaches zero, the performance is similar to IGME, but outperforms it slightly for low values of m.

2.3 Maximum-Likelihood Estimators

As demonstrated in [12] and the numerical results presented in Figure 2.2.2, a more efficient moment-based estimator can by found by taking the transformation $Y = R^{1/p}$ for any value of $p > 1$. Moreover, aymptotic series expansion for digamma function in $\Delta_{MLE} = \ln(m) - \psi(m)$ has the form identical to (2.9). Motivated by these observations, this section investigates the effects of transformation $Y = R^{1/p}$ on the development of approximate maximum-likelihood based estimators (AMLE) as well as optimization of coefficients polynomial approximations

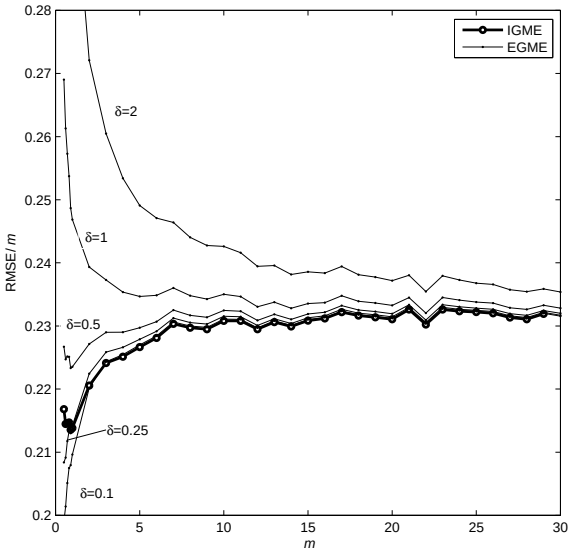

Figure 2.3: Exact estimators for the m parameter averaged over 100,000 independent estimates for a sample size $N = 50$.

for Δ_{MLE}. Letting $Y = R^{1/p}$ yields the likelihood function $\mathbf{L}$ as

$$\mathbf{L}(y_1, ..., y_N; m, \Omega) = \left[\frac{2p}{\beta^m \Gamma(m)}\right]^N \prod_{i=1}^{N} y_i^{2pm-1} \exp\left(\frac{-y_i^{2p}}{\beta}\right) \tag{2.15}$$

where $\{y_1, y_2, \ldots, y_N\}$ are samples of Y, and $\beta = \Omega/m$. Since maximizing $\ln(\mathbf{L})$ is equivalent to maximizing $\mathbf{L}$ itself, maximum likelihood estimates for β and m can be obtained by taking the derivative of $\ln(\mathbf{L})$ and setting them equal to zero, viz.,

$$\frac{\partial \ln(\mathbf{L})}{\partial m} = -N\ln(\beta) - N\psi(m) + \sum_{i=1}^{N} \ln(y_i^{2p}) = 0 \tag{2.16}$$

$$\frac{\partial \ln(\mathbf{L})}{\partial \beta} = -\frac{mN}{\beta} + \frac{1}{\beta^2}\sum_{i=1}^{N} y_i^{2p} = 0 \tag{2.17}$$

where $\psi(x) = \frac{\partial}{\partial x}\ln\Gamma(x)$ is the digamma function. It can be shown that likelihood equation has a unique solution which provides a maximum to (2.15). Solving (2.17) for β gives $\hat{\beta} = \left(\frac{1}{N}\sum_{i=1}^{N} y_i^{2p}\right)/m$. With $\hat{\beta}$ thus determined, $\hat{m}$ and $\hat{\Omega}$ can be solved iteratively as

$$\ln(\hat{m}) - \psi(\hat{m}) = \Delta_{MLE} = \ln\left[\frac{\frac{1}{N}\sum_{i=1}^{N} r_i^2}{\left(\prod_{i=1}^{N} r_i^2\right)^{1/N}}\right] \tag{2.18}$$

$$\hat{\Omega}_{MLE} = \frac{1}{N}\sum_{i=1}^{N} r_i^2 \tag{2.19}$$

respectively because $y_i = (r_i)^{1/p}$. Notice that Δ_{MLE} is independent of p and is identical to [11, Eq. (11)]. Thus variable transformation $Y = R^{1/p}$ does not yield a better maximum-likelihood estimation of m for larger values of p as it did for moment-based estimators. Furthermore, the maximum-likelihood estimator for Ω is simply $E\{R^2\}$, the mean sample power.

As in the GME case, a dilemma arises in solving the transcendental equation (2.18) as inverting (2.18) does not lend itself to a closed-form solution. Thus, [8], [11], [13, Eq. (6)], and [13, Eq. (7)] have resorted to asymptotic expansion of $\psi(\cdot)$ to derive an AMLE for m in closed form. Recognizing that the asymptotic series for Δ_{MLE} has the form identical to (2.9) and $0 < \ln(m) - \psi(m) < 1.27$, (2.9) can be used to approximate Δ_{MLE} to derive $\hat{m}$ in closed form. The final solution will be in the form of (2.10) and (2.12) except that Δ_{GME} is replaced with Δ_{MLE}, and coefficients c_0, c_1, and c_2 are optimized off-line separately.

Motivated by asymptotic series expansion, previous work on the subject of developing maximum-likelihood estimators have extended polynomial approximations only to the second order, viz. [11]. Because a simple method of inverting a cubic polynomial is known [16], a new estimator is developed by introducing a third term, viz.,

$$\Delta_{MLE} \approx c_0 + \frac{c_1}{m} + \frac{c_2}{m^2} + \frac{c_3}{m^3} \tag{2.20}$$

which can be written in the form $m^3 + a_1 m^2 + a_2 m + a_3 = 0$, where $a_1 = c_1/(c_0 - \Delta_{MLE})$, $a_2 = c_2/(c_0 - \Delta_{MLE})$, and $a_3 = c_3/(c_0 - \Delta_{MLE})$. Because the coefficients are optimized, the performance can only improve over known second-order AMLEs (e.g. if the expansion of $\Delta_{MLE} = \ln(m) - \psi(m)$ does not have a third polynomial term, the optimized coefficients will perform similarly to known second-oder approximations). In order to solve (2.20) for m, define $Q = (3a_2 - a_1^2)/9$ and $R = (9a_1a_2 - 27a_3 - 2a_1^2)/54$. It can be shown graphically that for the coefficients in Table 2.2 the descriminant $D = Q^3 + R^2$ is always positive when $0.5 \leq m \leq \infty$ $(0 < \Delta < 1.27)$, therefore (2.20) has three distinct real roots. Defining $S = (R + \sqrt{Q^3 + R^2})^{1/3}$ and $T = (R - \sqrt{Q^3 + R^2})^{1/3}$, these roots are [16]:

$$\hat{m_1} = S + T + \frac{1}{3}a_1 \tag{2.21}$$

$$\hat{m_2} = -\frac{1}{2}(S+T) - \frac{1}{3}a_1 - \frac{1}{2}\sqrt{-3}(S-T) \tag{2.22}$$

$$\hat{m_3} = -\frac{1}{2}(S+T) - \frac{1}{3}a_1 + \frac{1}{2}\sqrt{-3}(S-T) \tag{2.23}$$

From graphical observation, $\hat{m_1} \geq 0.5$, $\hat{m_2} < 0.5$, and $\hat{m_3} < 0$, therefore the only root of interest is always $\hat{m_1}$ and the others can be ignored. The coefficients are summarized in Table 2.2. The performances of these maximum-likelihood estimators are examined in Figures 2.4(b), 2.5, 2.6, and 2.7(b).

Table 2.2: Optimized coefficients for approximate maximum-likelihood estimators.

	c_0	c_1	c_2	c_3
AMLE-1	-5.9300E-3	5.8799E-1	-	-
AMLE-2	-5.0428E-4	5.0953E-1	6.5552E-2	-
AMLE-3	-5.5339E-6	4.9951E-1	8.7483E-2	-9.8577E-3

2.4 Bias Correction

Further improvements on estimates can be extended to simple bias correction methods which seek to fit the bias error exhibited in certain estimates to simple correcting functions. Because the bias for most estimators is approximately linear with respect to m and inversely proportional to sample size, an appropriate correcting function is

$$\hat{m}_{unbiased} = \hat{m}_{biased}\left(1 - \frac{c}{N}\right) \tag{2.24}$$

where c is a constant unique to each estimator which can be optimized offline. The benefits of this method are best observed in situations where bias error is a key issue. For estimators which exhibit little bias (such as AMLE-2 and AMLE-3 where the bias is less than 1% of m on average, see Figure 2.4(b)) the gains are negligible. In general, applying this bias correction method can reduce the estimator's RMS error of moment estimators by approximately 10%.

Table 2.3: Optimized coefficients for bias correction for several estimators for the Nakagami m-parameter

Estimator	c
AMLE-2	3.8230
AMLE-3	3.1667
AME_2-2	3.0343
$AGME_2$-2	3.1733
$AGME_3$-2	2.1767

2.5 Results and Discussions

The following comments and observations may be inferred from the Figures:

a) AME_3-2 based on lower order sample moments outperforms ME-AK and ME-CB although the latter are exact estimators for the m-parameter. This observation may be attributed to the fact that higher order sample moments are more susceptible to outliers particularly if the sample size is small;

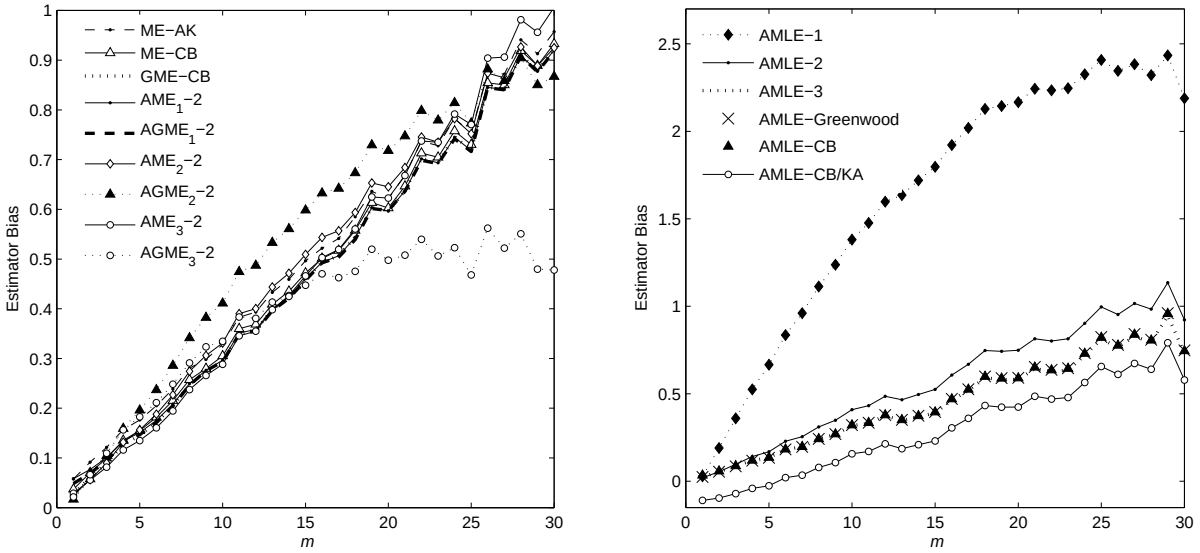

(a) Moment-based (25,000 independent trials)

(b) Maximum-likelihood based (5,000 independent trials)

Figure 2.4: Mean bias for several estimators plotted versus m for sample size $N = 100$.

b) The new AME_3-2 and AGME_3-2 estimators outperform ME-CB and GME-CB respectively for relatively small values of m in addition to having lower computational budget (involves the computation of only two sample moments). However, the difference between GME-CB and AGME_3-2 performance curves diminishes as the values for p and/or m increases;

c) AMLE-2 outperforms AMLE-CB/KA and AMLE-CB for relatively small values of m, but is comparable for larger values, especially with small sample sizes. Our Monte-Carlo simulation results also reveal that AMLE-2 possesses an accuracy close to the true maximum-likelihood estimator even at smaller values of m, and its performance is comparable to the classical result [13, Eq. (6)] due to Greenwood and Durand. Moreover, AMLE-2 is easier to implement compared to AMLE-Greenwood (i.e. $\hat{m}$ computed using (2.10) and (2.18) is continuous with respect to Δ_{MLE} and not piecewise continuous as given by [13, Eq. (6)]). The variances of AMLE-2 and AGME-2 are also smaller than AMLE-Greenwood at larger values of m;

d) Optimization in AME_2-2 and AGME_3-2 suppresses large RMS errors for low values of m, but at the slight expense of increasing error for higher m values. This is partially due to the unreliability of inverting the asymptotic nature of the ratio of two Gamma functions;

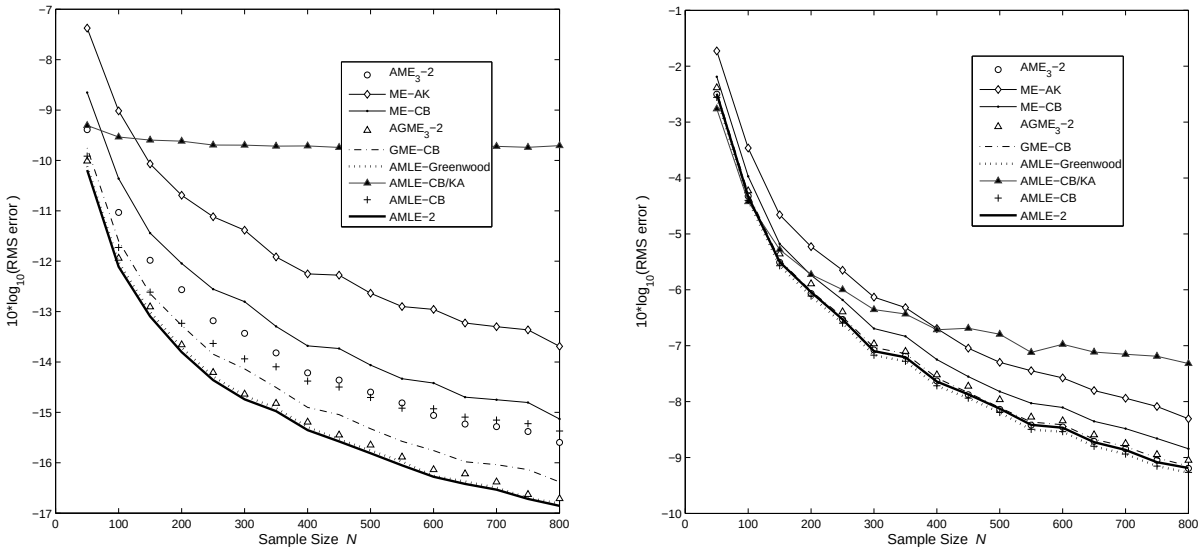

(a) $m = 0.5$ (b) $m = 2.5$

Figure 2.5: Logarithm of root mean-square error (averaged over 2,500 independent estimates) of different Nakagami-m parameter estimators plotted as a function of sample size N. The logarithm of RMS error was calculated to delineate superimposing plots at low error values.

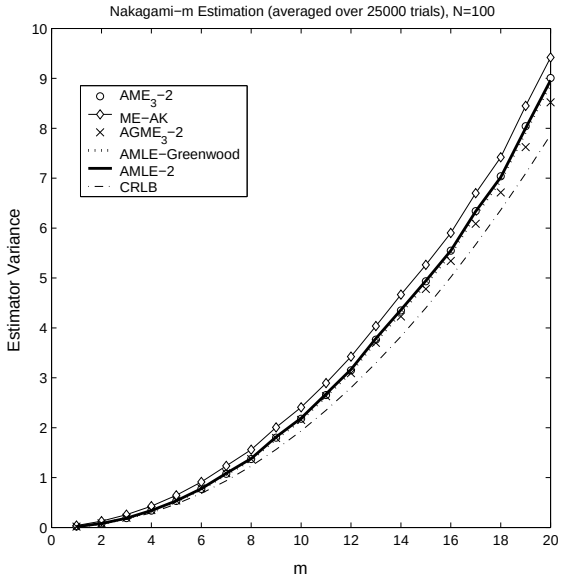

Figure 2.6: Variance of various estimators based on 25,000 experiments of $N = 100$ i.i.d. random variables plotted as a function of m.

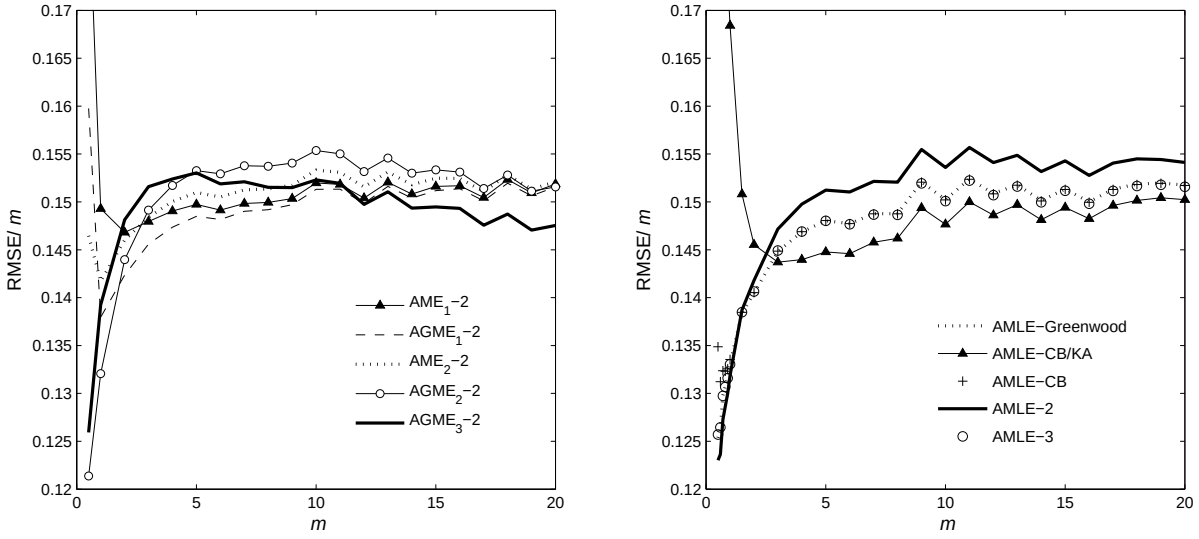

(a) Moment-based (50,000 independent trials)

(b) Maximum-likelihood (25,000)

Figure 2.7: Normalized root mean-square error (averaged over at least 25,000 independent estimates) of different 2^{nd}-order approximate Nakagami-m parameter estimators plotted against m for a sample size of $N = 100$

e) AMLE-3 performs as well as the best known maximum-likelihood estimator (Greenwood) without being piecewise continuous, thus preserving a relatively low computational complexity over a large range of m.

Although linear approximations for (2.5), (2.6), and (2.18) are grossly inadequate, quadratic and cubic polynomial approximations seem appropriate. An explanation for the large estimation error in AGME$_3$-1 (particularly for large values of p and m even with large sample size N) can be provided by noting that the right side of (2.6) approaches unity as p or m increases because $\lim_{x\to\infty} \frac{\Gamma(x+a)}{\Gamma(x)} e^{-a\ln x} = 1$, and hence the denominator in (2.12) approaches zero. Consequently, the estimator becomes more susceptible to small changes in Δ_{GME} (i.e. errors in the curve fitting become dominant as p gets larger. The AMLE-CB/KA also exhibits a similar trend, although the performance of this estimator improves for larger values of m.

Both AME$_1$ and AGME$_1$ perform relatively well over a broad range of m (preserving a sufficiently low variance without requiring coefficient optimization) and exhibit a slight performance improvement over the best known moment estimators for the m parameter [12, Eq. (6) and (9)] in addition to their lower computational complexity.

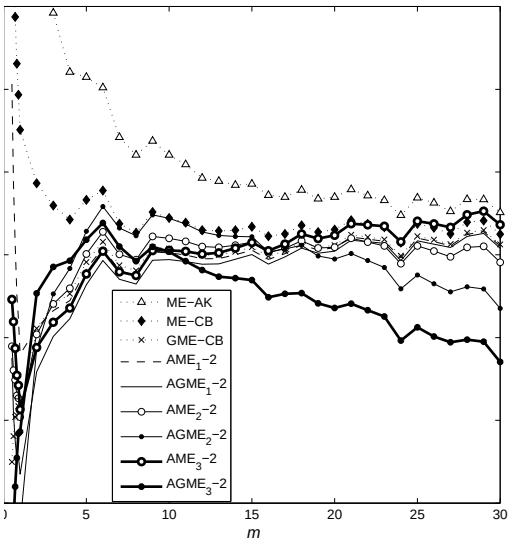

Figure 2.8: Normalized root mean-square error (averaged over 50,000 independent estimates) of different Nakagami-m parameter estimators plotted against m for a sample size of $N = 50$

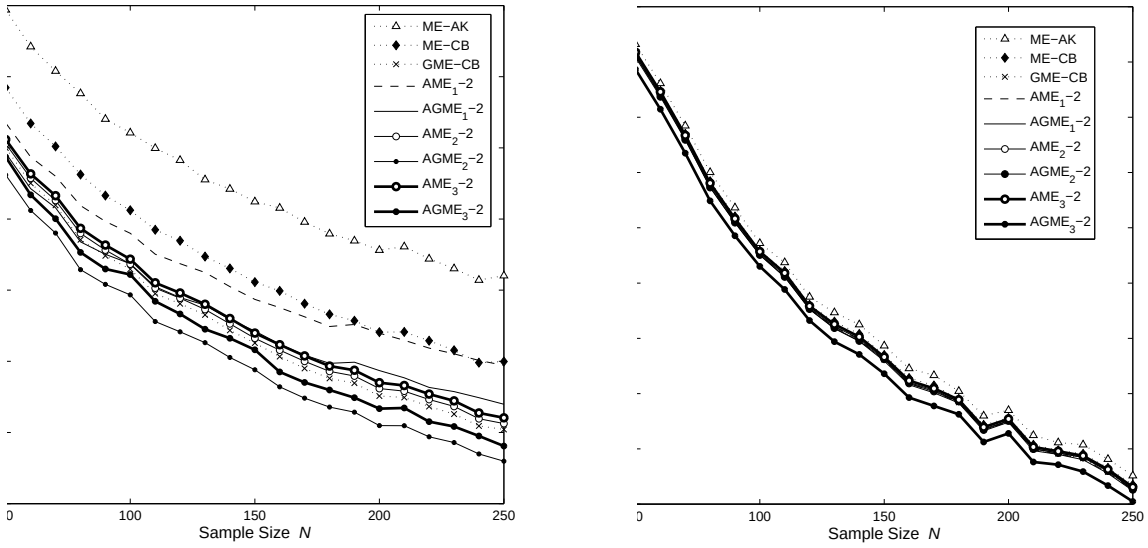

(a) $m = 0.75$ (b) $m = 20$

Figure 2.9: Logarithm of root mean-square error (averaged over 2,500 independent estimates) of different Nakagami-m parameter moment estimators plotted against sample size N. The logarithm of RMS error was calculated to delineate superimposing plots at low error values.

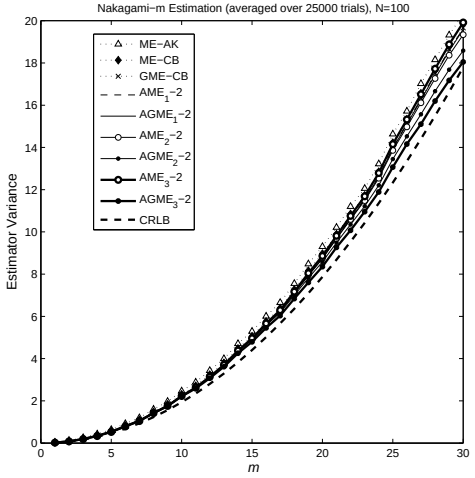

Figure 2.10: Variance of moment-based estimators calculated on 25,000 experiments of N=100 i.i.d. random variables plotted as a function of m

Table 2.4: Description of significant estimators used in this chapter for the Nakagami m-parameter.

Integer Moment-based Estimators	
AME$_1$-1*	Linear approximation to (2.5), coefficients determined by (2.7) and given in Table 2.1.
AME$_1$-2*	Quadratic approximation to (2.5), coefficients determined by (2.7) and given in Table 2.1.
AME$_2$-2*	Quadratic approximation to (2.5), coefficients optimized and given in Table 2.1.
AME$_3$-2*	Quadratic approximation to (2.6), coefficients optimized and given in Table 2.1.
ME-AK	[10, Eq. (5)]
ME-CB	[12, Eq. (4)]

Generalized Moment-based Estimators	
AGME$_1$-2*	Quadratic approximation to (2.5)for $p = 5$ coefficients determined by (2.7) and given in Table 2.1.
AGME$_2$-2*	Quadratic approximation to (2.5)for $p = 5$ coefficients optimized and given in Table 2.1.
AGME$_3$-2*	Quadratic approximation to (2.6)for $p = 5$ coefficients optimized and given in Table 2.1.
EGME$_\delta$*	Exact estimator given by (2.14)
GME-CB	[12, Eq. (9)]

Maximum-Likelihood based Estimators	
AMLE-2*	Quadratic approximation to (2.18), coefficients are optimized and given in Table 2.2
AMLE-3*	Cubic approximation to (2.18), coefficients are optimized and given in Table 2.2
AMLE-CB	[11, Eq. (10)]
AMLE-CB/KA	[11, Eq. (9)] or [8, Eq. (26)]
AMLE-Greenwood	[13, Eq. (6)]

* New estimators proposed in this chapter

Chapter 3

The Rice-K Channel

3.1 Introduction

Also known as the Nakagami-n distribution, the Rice-K multipath channel models a fading envelope by assuming a line of sight (LoS) component to the multipath elements summed at the receiver. The complex path gain at a particular frequency consists of a fixed (LoS) and a fluctuating (diffuse) components. When assuming a narrowband complex Gaussian stochasitc process, the time-varying envelope will exhibit a Rice distribution where the K factor is the power ratio of the LoS and diffuse components (often referred to in dB) and thus is commonly used to describe fading environments. The validity of the Rice-K distribution has been verified experimentally in [17] among others, and estimators have been proposed in [18], [19], [20], and [17].

This chapter presents several estimation techniques for the Rice K-parameter based on method of moments and proposes numerical approximations similar to those in Chapter 2. Furthermore, numerical methods are used to solve the maximum likelihood equation while no closed-form solution exists, and its performance is compared to existing estimators. In addition, several estimators for the Nakagami m-parameter are used for the K parameter by fitting the distributions to a well-known equation based on the second and fourth moments.

3.2 Moment Estimation

In Section 2.2 it was shown that while few closed-form solutions for moment estimators existed, appropriate moment estimators could be developed to overcome limitations seen through using higher-order moments. These appropriate generalized moment estimators use polynomial expansion approximations in order to invert transcendental equations while preserving low order moments. It was determined that although the estimators were only

approximations their performances were very close to theoretical. The performance of the Nakagami-m AGMEs motivates further investigation for similar estimation techniques for the Rice-K distribution.

Given a set of N i.i.d. random fading amplitude samples $\{r_1, r_2, \ldots, r_N\}$ drawn from a Rice-K distribution for instantaneous received signal amplitude, R,

$$f_R(r; K, \Omega) = \frac{2(K+1)r}{\Omega} \exp\left\{-K - \frac{(K+1)r^2}{\Omega}\right\} I_0\left(2r\sqrt{\frac{K(K+1)}{\Omega}}\right) \tag{3.1}$$

with average signal power $\Omega = E\{R^2\}$ and fading factor K, moment estimators attempt to estimate the fading parameters from sample moments. It is interesting to note that when $K = 0$ there is no LoS element and thus the received power exhibits a Rayleigh distribution. It is important to observe that this is the worst fading situation that the Rice distribution can describe which in itself is a limitation as empirical evidence suggests that under certain fading situations, particularly indoor mobile environments, the fading can be actually worse than Rayleigh. This is inherent to the nature of the Rice model which assumes a uniform distribution on AoA at the receiver for the reflected multipath components.

The k^{th} moment of the random fading amplitude in a Rice-K process is [20]

$$\mu_k = E\left\{R^k\right\} = \left(\frac{\Omega}{K+1}\right)^{k/2} \Gamma\left(\frac{k}{2}+1\right) e^{-K} {}_1F_1\left(\frac{k}{2}+1; 1; K\right) \tag{3.2}$$

where ${}_1F_1(a; b; x)$ is the confluent hypergeometric function of the first kind (see Appendix A) which can be expanded to a series polynomial. In certain conditions this expansion is finite, and thus closed-form moment estimators for K can be inverted. Such is the case with Tepedelenlioğlu et al. and the $\hat{K}_{2,4}$ estimator based on 2^{nd}- and 4^{th}- order moments. However recognizing that the process of modeling sample moments with a finite number with theoretical moments deviates for higher moment orders (primarily due to outliers) it is desirable to base estimation techniques on low-order moments. This, and the inherent success of Nakagami-m estimators in Section 2.2 is motivation to investigate the use of series expansion and approximations to ratios of moments for Rice-K estimators.

3.2.1 Approximate generalized moment estimators

It is obvious from the form of (3.2) that the ratio $\mu_{1/p}^2/\mu_{2/p}$ leads to a moment estimator for the K-parameter because the Ω term is eliminated. Furthermore it has been observed that the ratio of such Rice-K moments fits well to an inverted exponential polynomial, viz

$$\Delta = \frac{\mu_{1/p}^2}{\mu_{2/p}} \approx \exp\left\{\frac{1}{c_2K^2 + c_1K + c_0}\right\} \tag{3.3}$$

where c_0, c_1, and c_2 are coefficients that can be optimized offline for a specific value of p. Inverting (3.3) for K gives

$$\hat{K} = \frac{-c_1 - \sqrt{c_1^2 - 4c_2\left(c_0 - 1/\ln(\Delta)\right)}}{2c_2} \tag{3.4}$$

It is obvious from Figure 3.1 that the best estimator is based on μ_1^2/μ_2 (when $p = 1$). It is worth noting that fractional moments therefore do not improve Rice K-factor estimators as they did for Nakagami. For this reason, the $\hat{K}_{2,4}$ estimator will be the only approximate moment-based estimator discussed in this section.

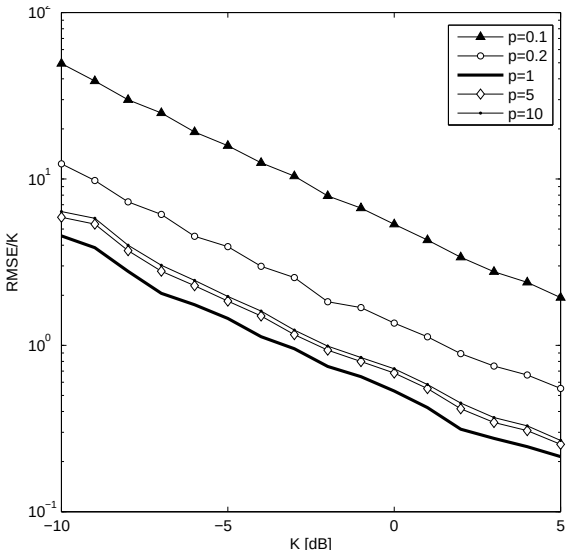

Figure 3.1: Root mean-square error for iterative solutions to generalized moment based estimators plotted vs. K for several values of p. The error was plotted on a log scale to delineate the curves for low error values.

For $p = 1$, the optimized values for c_0, c_1, and c_2 are -2.6057, -1.9583, and -6.5617E-4 respectively. Optimization was performed by fitting the right side of (3.3) to (3.4) in the minimum mean-square error sense using Quasi-Newton methods. The performance of the AGME can be seen in Figure 3.2.

3.3 Maximum Likelihood Estimation

The favorable results maximum likelihood estimation techniques have on Nakagami m-parameter estimators motives similar work on the Rice distribution. Given a set of N i.i.d. random variables $\{r_1, r_2, \ldots, r_N\}$ of received signal amplitude drawn from a Rice-K

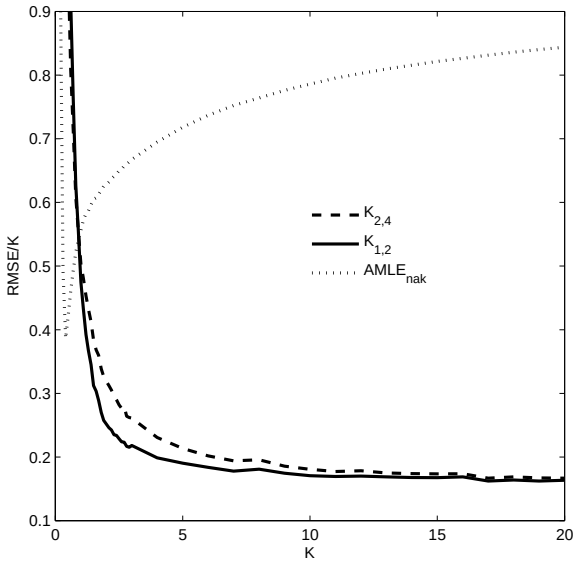

Figure 3.2: Normalized root mean-square error for approximate generalized moment estimators for the Rice K-factor.

distribution, the likelihood function $\mathbf{L}$ is

$$\mathbf{L}(r_1,\ldots,r_N;K,\Omega) = \prod_{i=1}^{N} \frac{2(K+1)r_i}{\Omega} \exp\left\{-K - \frac{(K+1)r_i^2}{\Omega}\right\} I_0\left(2r_i\sqrt{\frac{K(K+1)}{\Omega}}\right) \quad (3.5)$$

Finding the maximum of the $\ln(\mathbf{L})$ is equivalent to maximizing $\mathbf{L}$ itself, thus the log-likelihood function is

$$\mathbf{LLF} = \frac{1(K+1)}{\Omega}\sum_{i=1}^{N}\ln r_i - NK - \frac{K+1}{\Omega}\sum_{i=1}^{N} r_i^2 + \sum_{i=1}^{N}\ln\left[I_0\left(2r_i\sqrt{\frac{K(K+1)}{\Omega}}\right)\right] \quad (3.6)$$

Taking the derivative of (3.6)with respect to K and setting equal to zero gives

$$0 = \frac{N}{K+1} - \frac{2}{\Omega}\sum_{i=1}^{N} r_i^2 + \sum_{i=1}^{N}\frac{\frac{\partial}{\partial K}I_0\left(2r_i\sqrt{K(K+1)/\Omega}\right)}{I_0\left(2r_i\sqrt{K(K+1)/\Omega}\right)} \quad (3.7)$$

Solutions to the maximum-likelihood equation are difficult to formulate, primarily due to the last term in (3.7). Unlike Nakagami, however, the Rice maximum-likelihood equation has two solutions. One solution is always $K = 0$ and the second gives $\hat{K}_{ML}$, however this makes iterative convergence algorithms an issue, especially when K is small. For these reason solutions to (3.7) were not pursued.

3.4 Using Nakagami-m estimators for the Rice K-parameter

While estimators for the Rice K-parameter are difficult to develop, especially in closed-form, the distribution is similar in shape to other fading models, such as Nakagami. Therefore it is desireable to use existing estimators for these distributions for the Rice channel. Given random variables X_n and X_r with Nakagami-m and Rice-K distributions respectively, a relationship between the distributions' fading parameters can be made; observing Abdi and Kaveh's $\hat{m}_{2,4}$ Nakagami estimator [10] based on μ_2 and μ_4,

$$\frac{E^2\left\{X_n^2\right\}}{E\left\{X_n^4\right\}} = \frac{m}{m+1} \tag{3.8}$$

and Tepedelenlioğlu et al.'s $\hat{K}_{2,4}$ Rice estimator [20] based on the same moments,

$$\frac{E^2\left\{X_r^2\right\}}{E\left\{X_r^4\right\}} = \frac{(K+1)^2}{K^2+4K+2} \tag{3.9}$$

a relationship between m and K can be made by equating (3.8) and (3.9). Doing so and solving for K yields

$$K = 2m - 2 + \sqrt{m^2+m} \tag{3.10}$$

This solution makes sense, for when $m = 1$ the channel is experiencing Rayleigh fading which is the case for $K = 0$. Furthermore, the Rice distribution cannot account for situations where fading is worse than Rayleigh; where $m < 1$. This region gives a complex and meaningless value for K, thus m must be constrained to be no less than 1. The solution can also be inverted for m to give $m \approx (K+1)^2/(2K+1)$. The relationship between K and m can be seen in Figure 3.3. The Nakagami-m estimator AMLE-2 from chapter 2 was used for K-parameter estimation, the results of which can be seen in figure 3.2.

3.5 Numerical Results

The following results can be inferred from Figures 3.2, 3.3, 3.4, and 3.5:

a) The nature of $\hat{K}_{2,4}$ can present a problem when $\hat{\mu}_4 > 2\hat{\mu}_2^2$ as the estimator will return a complex number. This is often the case for low values of K where the 4^{th}-order moment is particularly susceptible to outlying samples. For the simulation complex or negative estimates were rejected and not considered in the RMSE calculation. For low values of K all estimates using $\hat{K}_{2,4}$ were rejected, as shown by Figure 3.2.

b) Fractional moments do not necessarily improve estimation for the Rice K-parameter as they did for the Nakagami m-parameter;

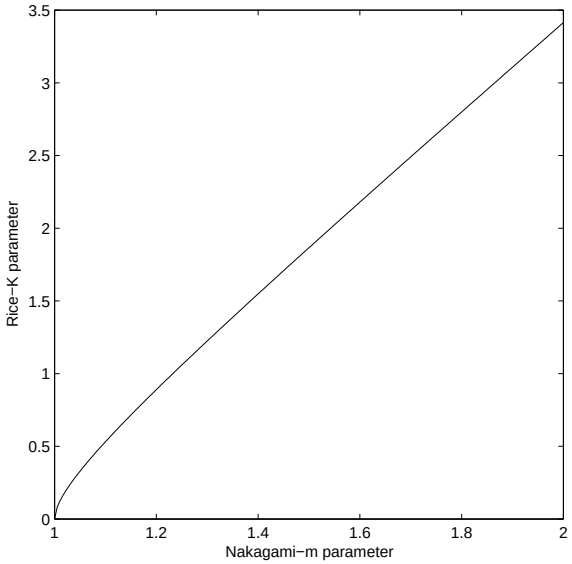

Figure 3.3: Nakagami-m fading parameter versus the Rice-K-parameter relation based on 2^{nd}- and 4^{th}- order moments.

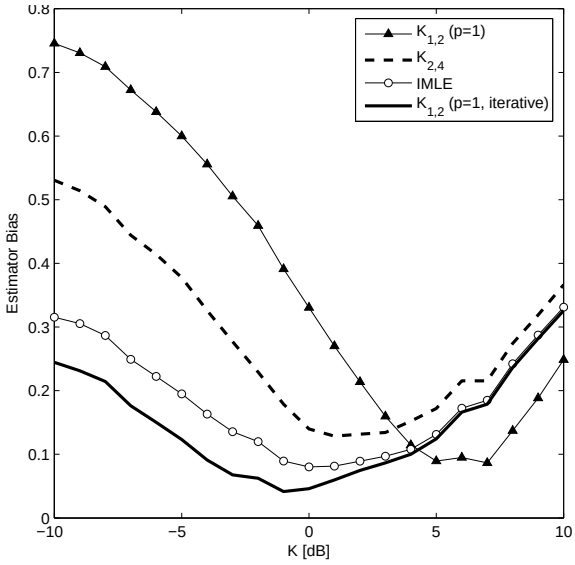

Figure 3.4: Bias for several Rice K-parameter estimators based on a sample size of N=100 and averaged over 10,000 independent trials

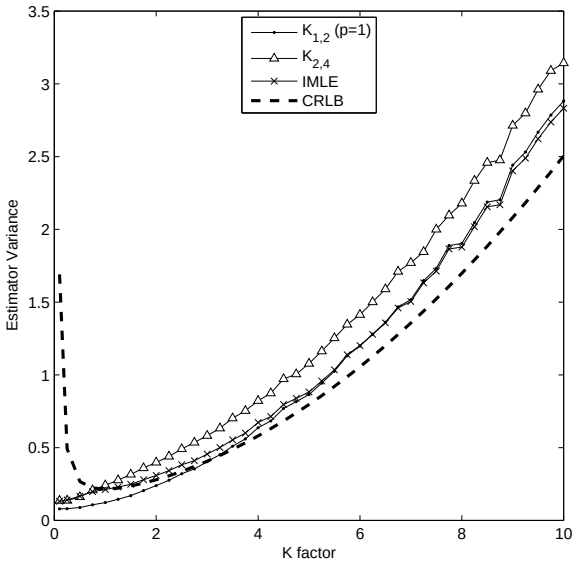

Figure 3.5: Estimator variance and the CRLB for several Rice-K estimators plotted vs. K and calculated on 10,000 independent experiments.

c) Although the error improvement $\hat{K}_{1,2}$ has over $\hat{K}_{2,4}$ is marginal, it produces fewer rejected estimates by being less prone to outliers, especially when K is small. Furthermore, the approximation given in (3.3) is appropriate;

d) Using Nakagami-m estimators for the Rice distribution is inherently limited by (3.10), but still provides a simple, closed-form solution, and outperforms $\hat{K}_{2,4}$ and $\hat{K}_{1,2}$ for small values of K;

Chapter 4

Weibull Estimators

4.1 Introduction

Intuitively, the efficacy such a model has on gauging channel quality is dependent upon the distribution chosen to describe the system. The Weibull distribution has not received as considerable attention as other fading models, such as Nakagami, Rice-K, and Rayleigh [12, 10, 19], despite its ability to describe experimental fading measurements in indoor [21] and outdoor [22, 23] environments [24, 25, 26]. Alouini and Simon proposed a generalized approach to diversity selection combining in channels subject to Weibull fading [27], while Sagias et al. investigated dual-branch switched-and-stay combining in receivers under such conditions in [28]. More recently, Cheng, Tellambura, and Beaulieu considered the effect knowledge of fading parameters has on Weibull slow-fading channels, including average bit error rates, outage probabilities, and several diversity combining schemes by developing a closed-form moment generating function for the distribution [29]. However, with exception to the aforementioned, limited results exist on the subject of Weibull fading channels.

Maximum likelihood estimation for Nakagami-m and Weibull distributions have been developed in [12], and [30] respectively. However, MLE are usually computationally intensive since it generally requires solving transcendental equations iteratively. For this reason moment estimators have been developed for Nakagami-m and Rice-K fading channel models. Noting that the ratio of integer and fractional (real) Weibull moments does not lead to closed-form solutions, Cran examined a modified moment estimator based on the difference between adjacent samples. While these estimators are heavily biased, a closed-form solution does exist. Percentile estimators have been discussed in [31] and references therein, however, a statistical comparison between various Weibull percentage estimators is not available in the literature.

This chapter describes several new estimators for the Weibull parameters that overcome some of the limitations proposed by previous related studies. These estimators are based

on fractional (real) moments, maximum-likelihood, adjacent-sample moments, percentile functions, and order statistics. In particular, many of these estimators are efficient and can be developed in closed form.

4.2 Generalized Moment Estimators

Moment-based estimators seek to estimate fading parameters α and β using sample moments of the random fading amplitude, defined as $\hat{\mu}_k = \frac{1}{N}\sum_{i=1}^{N} x_i^k$. Such estimation techniques are widely popular in the literature regarding a variety of fading models, yet limited results exist on the subject for Weibull distribution. This is likely due to the fact that no exact solution exists in closed-form, thus such estimators would resort to iterative solutions. In this section, a set of approximate generalized moment-based estimators (AGME) is proposed by expanding the ratio of Gamma functions to an invertible series. While only an approximation, the AGME performs only slightly inferior to solutions given by iterative methods, yet has a simple closed-form solution. Furthermore, two-step recursive estimator is developed that performs nearly as well as the iterative maximum-likelihood estimator which provides an empirical lower-bound to the root mean-square error for AGMEs.

4.2.1 Closed-Form Moment Estimation

Cheng and Beaulieu demonstrated in [12] that variable transformation $Y = X^{1/p}$ when applied to a Nakagami-m fading distribution improves the efficiency of its moment estimator. This is the motivation for creating a framework for estimating the Weibull fading parameter by admitting non-integer moments. It is also interesting to note that $Y = X^{1/p} \sim W(\alpha p, \beta^{1/p}), p > 0$ also has a Weibull distribution:

$$f_Y(y) = \frac{(\alpha p)}{(\beta^{1/p})^{(\alpha p)}} y^{\alpha p - 1} \exp\left\{ -\left(\frac{y}{\beta^{1/p}}\right)^{\alpha p} \right\} \tag{4.1}$$

which proves $Y \sim W(\alpha p, \beta^{1/p})$. From (4.1) the k^{th} moment of Y is given by

$$\mu_{k/p} = E\left\{Y^k\right\} = E\left\{X^{k/p}\right\} = \beta^{k/p}\Gamma(1 + \frac{k}{\alpha p}) \tag{4.2}$$

Note that (4.2) is not restricted to integers but is generalized to real moments as well. It is apparent from (4.2) that a ratio of moments can be chosen such that the β term is eliminated, viz

$$\Delta_{GME} = \frac{(\hat{\mu}_{1/p})^k}{\hat{\mu}_{k/p}} = \frac{\Gamma^k(1 + \frac{1}{\alpha p})}{\Gamma(1 + \frac{k}{\alpha p})} \tag{4.3}$$

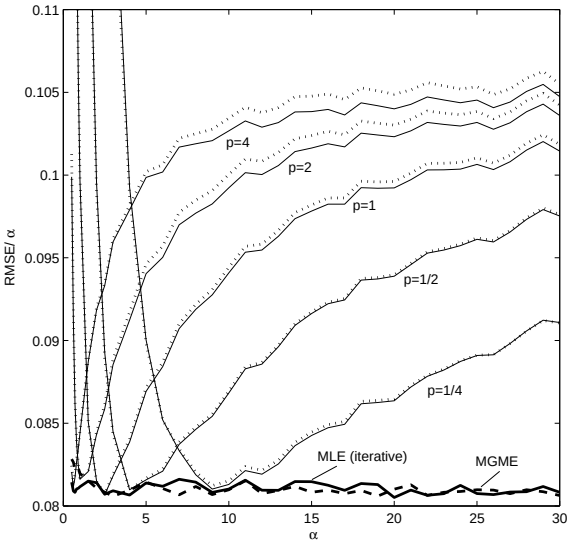

Figure 4.1: Normalized root mean-square error vs. α for $\text{AGME}_{2,p}$ for several different values of p

where k and p are arbitrary non-negative real numbers ($k \neq 1$), with sample moments defined as $\hat{\mu}_k = \frac{1}{N}\sum_{i=1}^{N} x_i^k$. A family of generalized-moment estimators based on k and p can be developed, however solving the transcendental equation for α can be cumbersome since no closed-form solutions exists. In practical implementation a closed-form expression for α is desired which motivates finding an approximate solution to (4.3). Iterative solutions to (4.3) can still be used to provide a benchmark against which approximate estimators can be compared. In these experiements iterative generalized moment estimators (IGME) use Newton-Raphson methods for α and are plotted in Figures 4.1 for several values of p with $k = 2$.

With knowledge of α closed-form estimator for β from (4.2) can be devised,

$$\hat{\beta}_{GME} = \left[\frac{\hat{\mu}_{1/p}}{\Gamma(1+\frac{1}{p\alpha})}\right]^p \tag{4.4}$$

which is identical to $\hat{\beta}_{ML}$ when $p = 1/\alpha$. Empirical evidence suggests that $\hat{\beta}_{ML}$ is the best estimator for β when $\alpha > 0.5$.

It has been observed that taking the inverted logarithm of the right side of (4.3) fits well to a quadratic polynomial, viz.

$$\Delta_{GME} \approx \exp\left\{\frac{1}{c_2\alpha^2 + c_1\alpha + c_2}\right\} \tag{4.5}$$

where the coefficients c_0, c_1 and c_2 can be optimized for a given pair of k and p. Such approximate generalized moment estimators (AGME) are referred to as $\text{AGME}_{k,p}$. Solving

the above equation for α gives

$$\hat{\alpha}_{GME} = \frac{-c_1 - \sqrt{c_1^2 - 4c_2(c_0 - 1/\ln \Delta_{GME})}}{2c_2} \tag{4.6}$$

The values of the coefficients for $\text{AGME}_{2,p}$ for several values of p can be found in Table 4.1. Optimization of the coefficients were performed with a Quasi-Newton method (i.e. curve fitting in a minimum-mean square error sense).

As demonstrated in Figure 4.1 moment-based estimators provide a reliable estimate of the Weibull parameters. Furthermore, Figure 4.1 shows that large error regions exist for sufficiently small values of α, and that empirically the lower bound for the performance of moment estimators is the (unbiased) maximum-likelihood estimator. Although iterative methods provide an exact solution, the $\text{AGME}_{2,p}$ perform nearly identically.

4.2.2 Modified Moment Estimation

Observing the RMSE trend of the generalized moment estimators in Figure 4.1, the region where the error is a minimum, the product αp is approximately a constant value. This trend arises from the fact that if $X \sim W(\alpha, \beta)$, then $Y = X^{1/p} \sim W(\alpha p, \beta^{1/p})$. This suggests that if p can be chosen appropriately, the estimator will achieve its minimum error by "reshaping" the samples to fit the estimator's low error region. However, a dilemma arises in the fact that initial knowledge of α is required to appropriately choose p. To circumvent this issue, a simple two-step process is proposed:

1. Use $\text{AMGE}_{2,1}$ to make a preliminary estimate (called α_x), despite the fact that the estimate may have considerable error.
2. Determine the optimum value of p by computing $p_{opt} = 2.5/\hat{\alpha}_x$, and perform variable transformation on the sample set $Y = X^{1/p_{opt}}$. Use $\text{AGME}_{2,1}$ again to obtain estimate $\hat{\alpha}_y$ from Y and divide by p_{opt} yielding $\hat{\alpha}_{opt}$.

Further iterations of this method could be used to assure convergence to the estimator's low error region, however simulations confirm that a single iteration yields results comparable to the maximum-likelihood estimator, see Figure 4.1. Furthermore, any AGME could be used, not just $\text{AGME}_{2,1}$. It is interesting to note that the modified generalized estimator (MGME) is efficient for low values of α despite the trend AGME has to higher error in this region. MGME is further improved by first correcting the bias introduced by $\text{AGME}_{2,1}$. Bias correction methods are described in section 4.7.1

Table 4.1: Optimized coefficients for integer and generalized moment-based Weibull α-parameter estimators

p	c_0	c_1	c_2
1/4	-4.5000E-2	-4.5000E-2	-4.9875E-3
1/2	-4.5000E-2	-4.5000E-2	-4.9875E-3
1	-4.5000E-2	-4.5000E-2	-4.9875E-3
2	-4.5000E-2	-4.5000E-2	-4.9875E-3
4	-4.5000E-2	-4.5000E-2	-4.9875E-3

4.3 Maximum Likelihood Estimators

Reliable and efficient maximum likelihood estimators (MLE) have been developed and extensively studied for a variety of fading distributions, including Weibull [30]. However due to the mathematical nature of the Weibull distribution, a closed-form solution to the shape parameter is not available, thus forcing estimates to rely on iterative solutions. Futhermore, the iterative MLE is positively biased, suggesting improvement through the use of bias-correcting algorithms.

As discussed in [12] and Section 4.2, a more efficient moment-based estimator can be found by taking the transformation $Y = X^{1/p}$ for certain values of p. This motivates investigation on the effects of taking the same transformation on maximum likelihood estimators. Letting $Y = X^{1/p} \sim W(\alpha p, \beta^{1/p})$ yields the likelihood function $\mathbf{L}$ as

$$\mathbf{L}\left\{y_1, y_2, \ldots y_N\right\} = \frac{\alpha p}{\eta^{1/p}} \prod_{i=1}^{N} y_i^{\alpha p - 1} e^{-y_i^{(\alpha p)}/\eta^{1/p}} \tag{4.7}$$

where $\{y_1, y_2, \ldots y_N\}$ are samples of Y and $\eta = \beta^\alpha$. Since maximizing $\ln(\mathbf{L})$ is equivalent to maximizing $\mathbf{L}$ itself, the maximum likelihood estimators for α and η can be solved by taking the respective derivatives of $\ln(\mathbf{L})$ and setting them equal to zero. The solution to $\hat{\eta}_{ML}$ is straight-forward and is $(1/N)\sum_{i=1}^{N} y^{(\alpha p)}$. With $\hat{\eta}_{ML}$ thus determined, $\hat{\alpha}$ and $\hat{\beta}$ can be solved iteratively as

$$\hat{\beta}_{ML} = \left[(1/N)\sum_{i=1}^{N} x^\alpha\right]^{1/\alpha} \tag{4.8}$$

$$\frac{1}{\hat{\alpha}_{ML}} + \frac{1}{N}\sum_{i=1}^{N} \ln(x_i) - \frac{\sum_{i=1}^{N} \ln(x_i) x_i^{\hat{\alpha}_{ML}}}{\sum_{i=1}^{N} x_i^{\hat{\alpha}_{ML}}} = 0 \tag{4.9}$$

because $y = x^{1/p}$. Notice that both $\hat{\eta}_{ML}$ and $\hat{\alpha}_{ML}$ are independent of p, thus variable transformation does not yield a better maximum likelihood estimator as it did for moment estimators. Furthermore, no closed-form solution exists for $\hat{\alpha}_{ML}$ and thus must be solved iteratively. Additionally, $\hat{\eta}_{ML}$ is dependent upon α. With perfect knowledge of α (greater

than 0.5) numerical resuls show that $\hat{\beta}_{ML}$ is very efficient (Cramér-Rao Lower Bound (CRLB) and $var\left[\hat{\beta}_{ML}\right]$ are nearly indiscernible), see Figure 4.6.

4.4 Moment Estimators Based on Adjacent Samples

In [32], Cran proposed an estimator based on moments defined by summing powers of differences between adjacent samples. The benefits to such estimators are realized by low-order moments and developing an estimator in closed form. Given a set of N ordered samples $\{x_1, x_2, \ldots, x_N\}$ drawn from a Weibull distribution, adjacent-sample moments are defined by

$$\bar{\mu}_k = \int_0^\infty \left[1 - F_X(x;\alpha,\beta)\right]^k dx = \frac{\beta}{k^{1/\alpha}}\Gamma\left(1+\frac{1}{\alpha}\right) \tag{4.10}$$

where $F_X(x)$ is the cumulative distribution function (CDF). It is obvious that the ratio of two adjacent-sample moments can lead to a family of estimators for α because the β term is eliminated. Furthermore, because the Gamma function's argument does not contain k as it did for (4.2), it is also eliminated, and the estimator can easily be written in closed form. Cran suggests the ratio $\bar{\mu}_1/\bar{\mu}_2$ as an estimator, and proposes a sample approximation to (4.10), viz.

$$\bar{m}_k = \sum_{i=0}^{N-1} \left[1 - MR_i\right]^k (x_{i+1} - x_i), x_0 = 0 \tag{4.11}$$

where x_i is the i^{th} sample, and MR_i is the median rank of the i^{th} sample. As demonstrated by Figure 4.2, however, the estimator is heavily biased. Most of this bias is likely due to the rectangular integral approximation, but also due to the poor approximation $MR_i \approx i/N$. The estimator can be further improved by admitting trapezoidal integration techniques (which do not greatly increase complexity), using a more accurate median rank approximation, and generalizing the ratio to any sample moments, not just $\bar{\mu}_1$ and $\bar{\mu}_2$.

The integral approximation in (4.10) using iterative rectangular methods will always undershoot the true integral due to the monotonically decreasing function $1 - F_X(x)$. This is the primary cause of the bias error seen in Figure 4.5. By admitting trapezoidal integration (4.11) can be improved;

$$\bar{m}_k = \frac{1}{2}\sum_{i=0}^{N-1} \left\{\left[1 - MR_i\right]^k + \left[1 - MR_{i+1}\right]^k\right\} (x_{i+1} - x_i), x_0 = 0 \tag{4.12}$$

and by using the improved median rank approximation $MR_i \approx (i - 0.3)/(N + 0.4)$ [33]. Higher-order numerical integration methods (such as Simpson's) are not advised as the samples $\{x_1, x_2, \ldots, x_N\}$ are not evenly separated. Although Simpson's integration technique is applicable to non-uniform sample spacing, it involves fitting group samples to a quadratic polynomial which can be severely misrepresentative of the underlying distribution, especially

for pairs of adjacent samples very close in value. Furthermore, higher-order numerical integration methods involve matrix inversions to solve for the polynomial coefficients which are often, among other things, computationally tedious and thus undesirable, thus the benefits of linear (trapezoidal) integration are apparent.

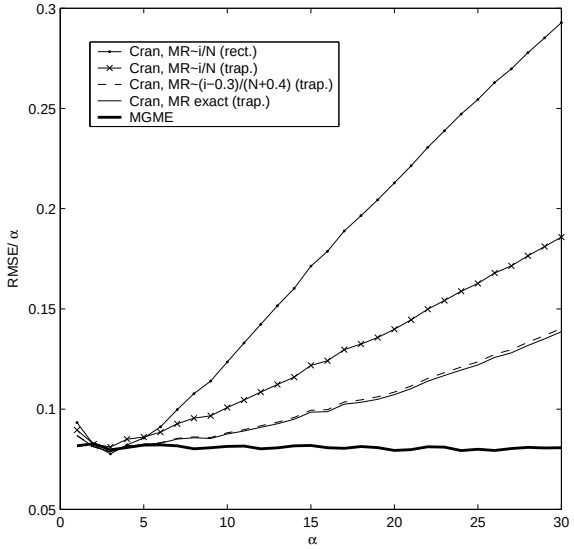

Figure 4.2: Normalized root mean-square error for several variations of Cran's estimator calculated on 5,000 independent trials and plotted versus α for sample size $N = 100$.

From hereon the modified Cran estimator with trapezoidal integration and improved median rank calculation will be referred to as MC, the benefits of which can be seen in Figure 4.2. Furthermore we can develop a more generalized estimator based on Cran's framework by admitting generalized moments. Solving $\bar{\mu}_{k_1}/\bar{\mu}_{k_2}$ for α yields

$$\hat{\alpha} = \frac{\ln(k_2/k_1)}{\ln(\bar{m}_{k_1}/\bar{m}_{k_2})} \tag{4.13}$$

which is identical to Cran's estimator when $k_1 = 1$ and $k_2 = 2$. Experimental testing suggests the best results are achieved when k_1 and k_2 are almost identical and close to 1. Thus, an estimator with $k_1 = 1$ and $k_2 = 1+1/p$ for any positive p is devised and denoted MC_p. Figure 4.4 demonstrates the benefits achieved from admitting non-integer moments for estimators utilizing moments based on adjacent samples. The estimator improves as p increases, but only up to a limit.

4.5 Percentile Estimators

Percentile estimators for the Weibull distribution have been discussed in [31] and references therein, however optimized coefficients specific to the shape parameter are needed, thus either

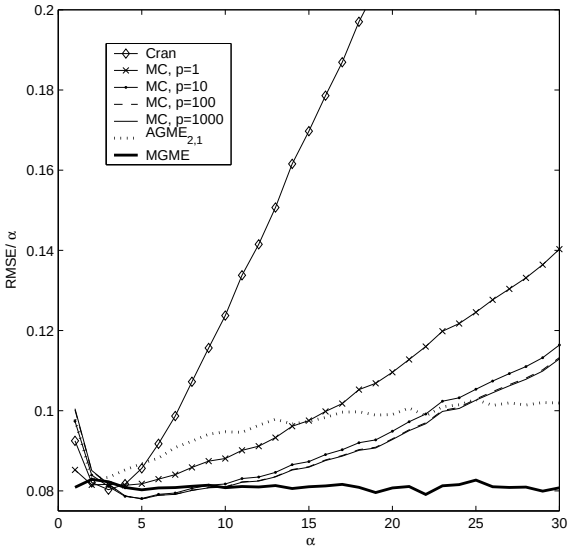

Figure 4.3: Normalized root mean-square error for several generalized modified Cran (MC) estimators calculated on 10,000 independent trials and plotted versus α for sample size $N = 100$. All modified Cran estimators use trapezoidal numerical integration as well as approximate median rank $\frac{i-0.3}{N+0.4}$

a moderate set of coefficients whose performance is good for a broad range of α are accepted, or some sort of iterative method or lookup table is required. Furthermore, the estimators are heavily biased. This section develops a new percentile estimator that is efficient and does not require initial knowledge of channel parameters.

Given an ordered set of R.V., $\{x_{1:N}, x_{2:N}, \ldots, x_{N:N}\}$, percentile estimators attempt to map the sample set to the distribution's cumulative distribution function (CDF). One of the features of the Weibull distribution is its uniquely invertible CDF,

$$F_X(x) = 1 - e^{-(x/\beta)^\alpha} \tag{4.14}$$

thus it is possible to develop a simple closed-form estimator for α based on percentile statistics. For a given probability $F_X(x) = p_k$, the corresponding sample value is

$$x_k = \beta \left[\ln(1 - p_k)\right]^{1/\alpha} \tag{4.15}$$

For a given pair of probabilities (p_1, p_2), we can devise a simple estimator based on the ratio of $x_{n_1:N}/x_{n_2:N}$ where $x_{n_i:N}$ is the sample closest to $p_i N$. This ratio leads to the estimator

$$\hat{\alpha}_{p_1,p_2} = \frac{\ln\left[\ln(1-p_1)/\ln(1-p_2)\right]}{\ln\left(x_{n_1:N}/x_{n_2:N}\right)} \tag{4.16}$$

which will hereafter be referred to as PE_{p_1,p_2}. The estimator is similar to that originally proposed by Schmid, however relying only on two percentiles rather than three, primarily

because of the different in the underlying distributions; Schmid attempted to make estimations on a 3-parameter distribution by solving three separate equations simultaneously, thus requiring a third value. The performance for the shape parameter, as a result, suffered, however this section makes no claims on estimation techniques of the threshold parameter.

Although a closed-form percentile-based estimator have been described by (4.16), appropriate values of p_1 and p_2 have yet to be determined. Interestingly, the relative RMSE is independent of the pair chosen. That is, the error does not exhibit the high/low trends that AGMEs and IGMEs do, but rather is linear with respect to α, much like MLE and MGME (see Figure 4.1). A systematic approach based on Monte Carlo simulations confirms that the optimal values of p_1 and p_2 are about 0.17 and 0.96 respectively. Although estimators based on three (or more) percentiles can be developed in closed form using this framework, it was found that the improvement upon PE_{p_1,p_2} was only slight, and the optimal values for additional probabilities (p_3, p_4, etc.) converge to that of p_1 and p_2. The results for $\text{PE}_{0.17,0.96}$ can be found in Figure 4.4(b).

The approximation $p_i \approx F_{n_i:N}(x_{n_i:N})$ is the cause of some error when sample size is low. In this case it is improbable that the sample $x_{n_i:N}$ is actually close to $p_i N$, thus the an appropriate median rank approximation $\tau_i = (n_i - 0.3)/(N + 0.4)$ [33] can replace p_i in (4.16). Although the estimator does exhibit a slight bias, it is only marginal, and independent of β, thus simple bias-correcting methods for PE_{p_1,p_2} can be used.

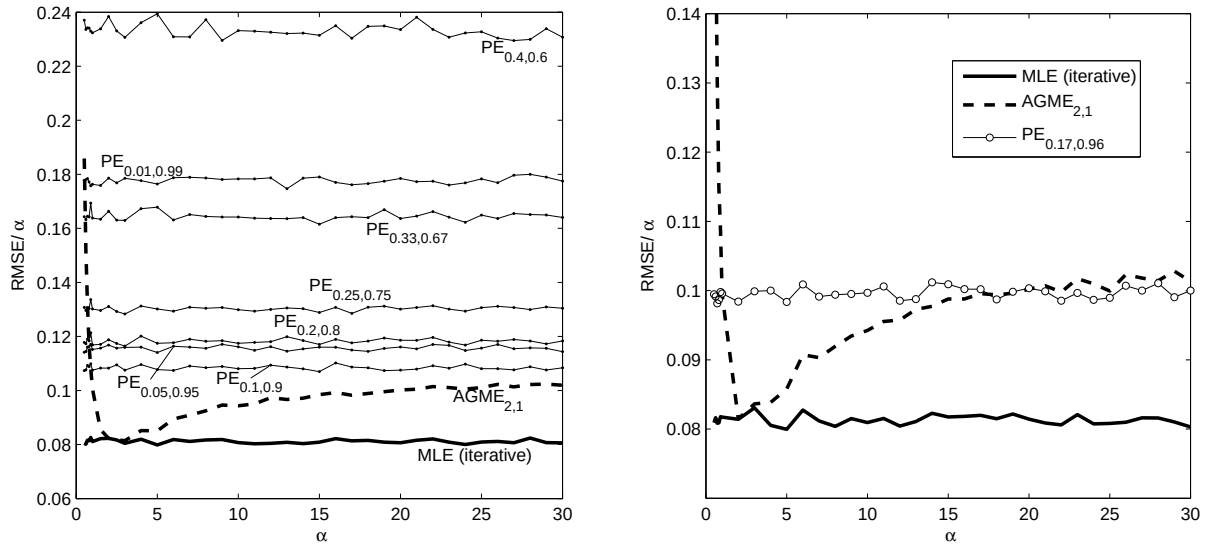

(a) $\text{PE}_{p,1-p}$ (b) $\text{PE}_{0.17,0.96}$

Figure 4.4: Normalized root mean-square error for Weibull percentile estimators for averaged on 10,000 independent trials and plotted versus α for a sample size of $N = 100$.

4.6 Estimators Based on Order Statistics

This section investigates estimators based on order statistics. Although these estimators are expected be inferior to the others presented in this paper, they still provide a simple closed-form solution and therefore merit discussion. Given a set of N i.i.d. ordered random samples $\{x_1, x_2, \ldots, x_N\}$, the k^{th} order statistic is given by [14, Eq. (7-14)]

$$f_{k:N}(x_{k:N}) = \binom{N}{k} \left[1 - F_X(x)\right]^{k-1} F_X(x)^{N-k} f_X(x) \tag{4.17}$$

where $F_X(x)$ and $f_X(x)$ are the cumulative distribution and probability density functions of $X \sim W(\alpha, \beta)$ respectively. From (4.17) the PDF for the minimum order Weibull statistic can be easily written as

$$f_{1:N}(x_{1:N}) = \alpha \left(\frac{N^{1/\alpha}}{\beta}\right)^{\alpha} x_{i:N}^{\alpha-1} \exp\left\{\left(\frac{x_{i:N} N^{1/\alpha}}{\beta}\right)^{\alpha}\right\} \tag{4.18}$$

which itself has a Weibull distribution, $X_{1:N} \sim W(\alpha, \beta/N^{1/\alpha})$. Therefore, its expected value is

$$E\left\{X_{1:N}\right\} = \frac{\beta}{N^{1/\alpha}} \Gamma\left(1 + \frac{1}{\alpha}\right) \tag{4.19}$$

A simple estimator can therefore be developed for the shape parameter based on the ratio of the minimum sample's expected value and the first moment of the sample vector, viz.

$$\Delta_{1:N} = \frac{E\left\{X_{1:N}\right\}}{E\left\{X\right\}} = \frac{1}{N^{1/\alpha}} \tag{4.20}$$

Solving for α gives

$$\hat{\alpha_{1:N}} = \frac{\ln(N)}{\ln\left(\mu_1 / x_{1:N}\right)} \tag{4.21}$$

Evaluating the Fisher Information [14, Eq. (8-97)] of this estimator explains its inferior performance to moment-based estimators; any order statistic does not hold much information about shape parameter as it is based on one sample alone, and thus will be inferior to any moment-based estimator. This is not the case for all parameters, however, and an exception can be seen when attempting to estimate the threshold parameter as done in [31] with percentile estimators.

4.7 Numerical Results

4.7.1 Bias Correction

As made evident by Figure 4.5 many of the estimators discussed in this paper demonstrate some sort of bias. In effort to minimize estimation error, we propose a bias-correction method

via curve-fitting to an appropriate expression. For many estimators for the shape parameter, the bias varies linearly with α, inversely with sample size, and is independent of β. Therefore an approximate unbiased estimator on a set of N samples can be written as

$$\hat{\alpha}_{unbiased} = \hat{\alpha}_{biased}\left(1 - \frac{c}{N}\right) \tag{4.22}$$

where c is a constant coefficient optimized for each estimator. Optimized values can be found in Table 4.2. Generally applying this unbiasing method to such estimators has up to a 10% improvement on the root mean-square estimation error.

The bias for location parameter (β) estimators is dependent upon not only sample size and β itself, but α as well, thus a more complex correcting function would need to be developed. The bias for β, however, is only an issue for values of $\alpha < 1$ for which the distribution's PDF, $f_X(x)$ has an asymptote at $x = 0$. This is range of α is generally impractical for modeling communications systems, therefore the bias error in this region exhibited by $\hat{\beta}$ may be ignored.

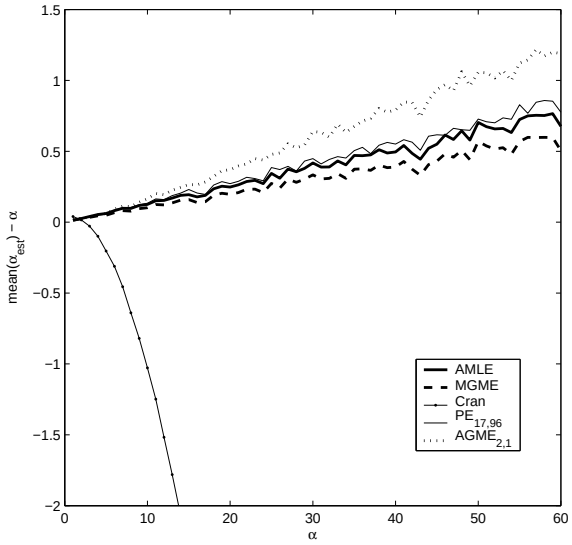

Figure 4.5: Bias of several estimators for α averaged over 100,000 independent experiments for a sample size of $N = 100$

4.7.2 Cramér-Rao Lower Bound

The variance of an estimator is crucial in evaluating its performance as it demonstrates an estimator's ability to perform reliably. For an unbiased estimator, a lower limit of its variance is governed by the Cramér-Rao Lower Bound. To calculate the bound, it is necessary to first

Table 4.2: Coefficients for α-Estimator Bias Correction

Estimator	c
MGME	0.93956
IMLE	1.22506
$\text{PE}_{17,96}$	1.34499
$\text{AGME}_{2,0.25}$	1.74371
$\text{AGME}_{2,0.5}$	1.91483
$\text{AGME}_{2,1}$	2.03745
$\text{AGME}_{2,2}$	2.08041
$\text{AGME}_{2,4}$	2.09471

evaluate the Fisher Information [14, Eq. (8-97)], viz.

$$I(\theta) = -E\left\{\frac{\partial^2}{\partial\theta^2}\ln f_X(x;\theta)\right\} \tag{4.23}$$

where θ is the parameter we desire to estimate. The variance of an unbiased estimator $\hat{\theta}$ on N i.i.d. samples must be greater than or equal to $[NI(\theta)]^{-1}$. After considerable mathematics, the CRLB for α can be written as

$$\text{CRLB}\left[\hat{\alpha}\right] = \frac{1/N}{\frac{1}{\alpha^2} + \int_0^\infty \frac{\alpha x^{2\alpha-1}}{\beta^{2\alpha}}\ln^2\left(\frac{x}{\beta}\right)e^{-(x/\beta)^\alpha}dx} \tag{4.24}$$

CHECK!!! Evaluating the integral in the denominator is difficult, however numerical approximations confirm that that variance increases similarly to a quadratic polynomial, therefore curve-fitting to the numerical calculation of the CRLB for α gives a good approximation:

$$\text{CRLB}\left[\hat{\alpha}\right] \approx \frac{0.5484\alpha^2 - 0.001941\alpha + 0.01003}{N} \tag{4.25}$$

This approximation is very good for values of $\alpha > 1$, but is slightly optimistic for smaller values. Still, (4.25) provides a reliable and fast lower bound and is used instead of numerical solutions to (4.24) in the Figures. The CRLB for β is easily derived to be

$$\text{CRLB}\left[\hat{\beta}\right] = \frac{\beta^2}{N\alpha^2} \tag{4.26}$$

however proving that $\hat{\beta}_{ML}$ achieves this is difficult as deriving an expression for its variance is not trivial (an estimator is said to be efficient if its variance is equal to the CRLB). In lieu of this dilemma, we again substitute $\eta = \beta^\alpha$. The CRLB for η is simply

$$\text{CRLB}\left[\hat{\eta}\right] = \frac{\eta^2}{N} \tag{4.27}$$

Furthermore, $Y = X^\alpha \sim W(1, \eta)$ is exponentially distributed with mean η and variance η^2. Exploiting the Central Limit Theorem [14] in (4.8), $\hat{\eta}_{ML} \sim N(\eta, \eta^2/N)$ as $N \to \infty$. Due to the shape of the PDF of Y (exponential), the approximation of $\hat{\eta}_{ML}$ to have a normal distribution is very good, even for relatively small N, thus (4.8) has a variance equal to its CRLB and is therefore asymptotically efficient as sample size increases. Assuming perfect knowledge of α, $\hat{\beta}_{ML} = \hat{\eta}_{ML}^{(1/\alpha)}$ is also asymptotically efficient and has a variance given by (4.26), but only for values of α greater than 1. Empirical evidence in Figure 4.6 supports this claim.

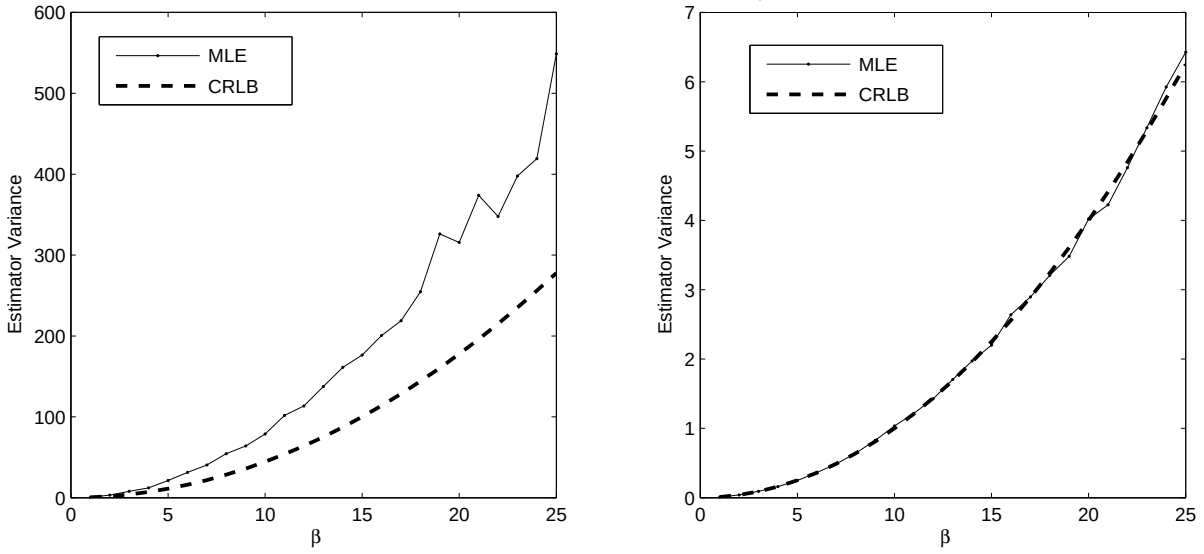

(a) $\alpha = 0.15$ (b) $\alpha = 1$

Figure 4.6: Variance for the maximum-likelihood estimator for β calculated on 5,000 independent estimates for a sample size of $N = 100$ versus β.

The following comments and observations may be inferred from the Figures:

a) Iterative solutions to (4.9) provides an empirical lower bound to the RMS error for iterative and approximate GMEs. Furthermore, by reshaping the distribution to fit the low error region of $\text{AGME}_{k,p}$, MGME performs almost identically to the iterative MLE while preserving a low computational complexity;

b) Cran's estimator based on adjacent-sample moments can be vastly improved by using trapezoidal integration and a better median rank function which are realized in Figure 4.2, and by admitting generalized moments (Figure 4.4). The bias error in MC_p due to numerical integration is greatly reduced, however is still present, and is inferior to $\text{AGME}_{k,p}$ for large values of α;

c) Estimators based on percentile and order statistics provide simple, closed-form solutions for α, however are inferior to moment methods;

d) Bias error is a concern for all estimators, especial for the location parameter, β, when α is small;

Table 4.3: Description of significant estimators used in this chapter for the Weibull α-parameter.

Generalized Moment-based Estimators	
AGME$_p$*	Quadratic approximation to (4.3), $k = 1$, coefficients are optimized and given in Table 4.1
IGME$_p$*	Iterative solution to (4.3), $k = 1$
MGME*	Modified estimator using recursive method to solve for optimal p value, giving low RMS error
Adjacent-sample Moment-based Estimators	
Cran	[32] Original estimator based on adjacent-sample moments
MC*	Modified version of Cran's estimator using improved median rank approximation and trapezoidal numerical integration
Other Estimators	
IMLE	Iterative maximum-likelihood solution to (4.9)
PE$_{p_1,p_2}$	Percentile estimator given by (4.16). Optimal values for p_1 and p_2 are 0.17 and 0.96 respectively
$\hat{\alpha}_{1:N}$	Estimator based on minimum sample and μ_1, given by (4.21)

* New estimators proposed in this chapter

Chapter 5

Applications in Adaptive Radios

5.1 Introduction

Adaptive modulation is a technique being incorporated into a growing population of wireless radios, however a key requirement to the performance of adaptive modulation is to accurately measure the channel's fading characteristics. In a typical situation the signal amplitude consists of quickly changing power fluctuations due to multipath signal combining at the receiver as well as long-term variations primarily due to shadowing. Adaptive modulation attempts to mitigate the effects fading has on narrowband wireless systems by exploiting the BER characteristics of different modulation types, however little work exists on the topic to incorporate fading models other than Rayleigh [34, 35] due to the difficulty in solving equations numerically and computing complex integrals. As a result, many systems resort to assuming a Rayleigh distribution which for outdoor environments is often pessimistic and cannot utilize the true bandwidth of the channel. Empirical evidence [36] also shows that indoor propagation poorly fits the Rayleigh distribution and often includes situations where fading is worse than Rayleigh, thus the benefits of more accurately describing the channel are transparent.

This chapter investigates the effects channel knowledge has on adaptive modulation schemes as well as developing BER approximations in AWGN channels in order to develop a unified expression under certain fading situations. Furthermore, an approximate upper bound on BER performance for adaptive switching modulation systems in fading channels is devised, extending Torrance and Hanzo's work in [34, 35] to include a variety of fading situations, including Nakagami-m, Nakagami-q, and Rice-K. Finally, an adaptive switching modulation system for a channel undergoing fast-fading is simulated, the performance of which is characterized by matching to the slowly-changing shadowing component and compared to systems where only basic assumptions are made about the fading characteristics of the channel.

Table 5.1: Optimized coefficients for approximate BER for M-ary PSK and M-ary QAM in AWGN channels.

	Approx. 1 (5.1)		*Approx. 2* (5.2)		
M-PSK	a	b	a	b	c
2	2.7106E-1	1.1348E+0	1.6214E-1	1.0645E+0	1.9975E-1
4	2.9447E-1	5.7870E-1	8.9403E-4	2.9904E-1	2.8202E-1
8	1.8077E-1	1.6402E-1	1.0267E-1	1.5510E-1	1.6718E-1
16	1.4015E-1	4.3021E-2	7.1904E-2	3.9760E-2	1.2993E-1
32	1.1214E-1	1.0903E-2	6.1306E-2	1.0160E-2	9.7244E-2
M-QAM	a	b	a	b	c
16	2.5072E-1	1.1791E-1	1.1002E-1	1.0541E-1	2.1261E-1
64	2.4310E-1	2.9183E-2	8.2198E-2	2.5002E-2	1.8771E-1
256	2.0793E-1	7.2933E-3	6.2349E-2	6.1622E-3	1.9314E-1

5.2 Effects of Fading on M-ary QAM/PSK Channels

This section investigates the effects channel fading at the receiver has on uncoded narrowband wireless modulation schemes. Perfect coherent detection is assumed and thus all results are upper-bound limited due to received power only.

5.2.1 Approximate bit error rates for PSK/QAM in AWGN channels

Given the familiar waterfall curve nature of the the bit error rates (BER) for M-ary QAM/PSK in additive white Gaussian noise (AWGN) channels, a pair of approximations with certain special properties can be used, viz.

$$P_e \approx ae^{-b\gamma} \tag{5.1}$$

$$P_e \approx ae^{-b\gamma} + ce^{-2b\gamma} \tag{5.2}$$

where P_e is the target bit error rate (BER) for a given channel SNR (γ). These forms are particularly appealing due to their ability to be uniquely invertible for γ. This suggests that for a desired QoS a particular required E_s/N_0 (γ_{req} can be uniquely determined given a modulation type in an AWGN channel. Solving for this signal power gives

$$\gamma_{req} \approx -\frac{1}{b}\ln\left(\frac{P_e}{a}\right) \tag{5.3}$$

$$\gamma_{req} \approx -\frac{1}{b}\ln\left(\frac{-a+\sqrt{a^2+4cP_e}}{2c}\right) \tag{5.4}$$

While there exist better approximations, the choice for (5.1) and (5.2), aside from being easily invertible for γ will be apprent when fading channel models are considered. The coefficients for M-ary QAM and M-ary PSK were optimized on a log-log scale (as in Figure 5.1) in the minimum mean-square error sense using Quasi-Newton methods and can be found in Table 5.2.1. The fit performance to the true BERs for M-ary QAM and M-ary PSK can be seen in Figure 5.1.

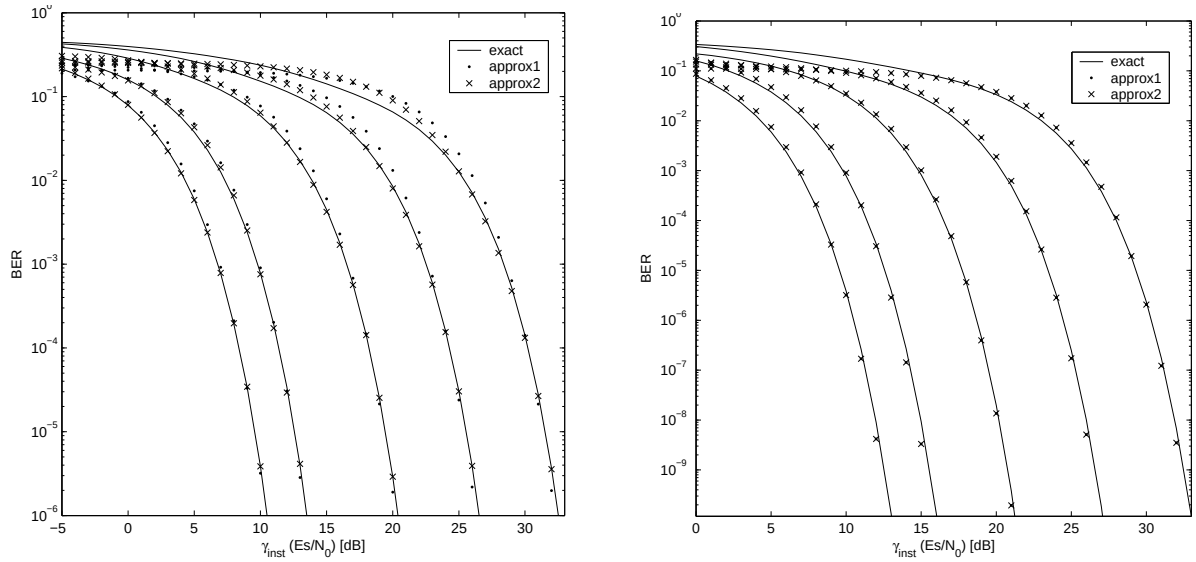

(a) M-ary QAM (2, 4, 16, 64, 256)

(b) M-ary PSK (2, 4, 8, 16, 32)

Figure 5.1: Exact and approximate bit error rates for instantaneous channel SNR (E_s/N_0) for AWGN channels.

5.2.2 Approximate BER for M-ary PSK/QAM in fading channels

Given a fading distribution $f_\gamma(\gamma;\Omega)$ for instantaneous received signal power γ and with average power Ω, the upper bound for the average bit error rate for a modulation scheme can be calculated by averaging its instantaneous BER performance over the distribution, viz.

$$\bar{P}_M(\Omega) = \int_0^\infty P_M(\gamma) f_\gamma(\gamma;\Omega) d\gamma \tag{5.5}$$

Given the BER approximation given by (5.1) in section 5.2.1, (5.5) reduces to

$$\begin{aligned} \bar{P}_M(\Omega) &\approx \int_0^\infty a e^{-b\gamma} f_\gamma(\gamma;\Omega) d\gamma & (5.6) \\ &\approx a\Phi(b\Omega) & (5.7) \end{aligned}$$

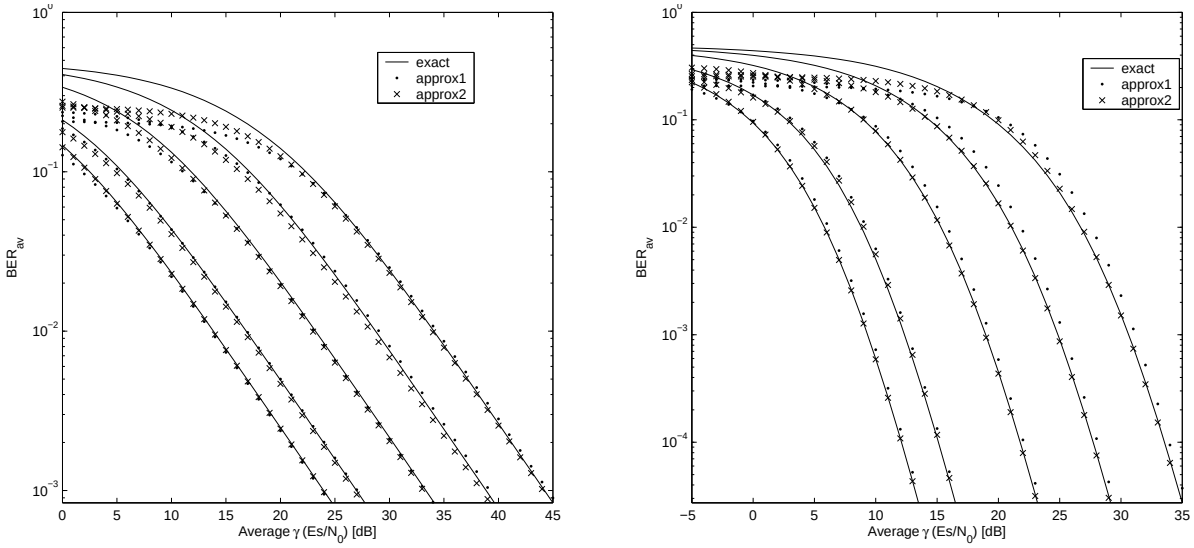

(a) $m = 1$ (b) $m = 5$

Figure 5.2: Exact and approximate average BER for M-ary QAM channel ($M = 2, 4, 16, 64, 256$) undergoing Nakagami-m fading.

where $\Phi(s)$ is the moment generating function of the fading distribution. In essence the integral acts as the Laplace transform of the distribution and in some cases can be uniquely inverted for a required average signal power Ω. This is especially useful when the target BER is desired for a specific modulation scheme, however knowledge of the channel's fading statistics are required, hence the emphasis on accurate and efficient parametric estimation of the fading parameters. In the case of Nakagami-m fading, for example, the approximate average bit error rate is

$$\bar{P}_M(\Omega; m) = a \left[\frac{m}{m + b\Omega} \right]^m \tag{5.8}$$

Thus, the required average received signal power to achieve an average BER of $\bar{P}_M$ is approximately

$$\Omega_{req} = \frac{m}{b} \left[\left(\frac{\bar{P}_m}{a} \right)^{-1/m} - 1 \right] \tag{5.9}$$

The results of the approximations due to (5.1) and (5.2) can be found in Figure 5.2. It is evident from this Figure that the approximations are best when m and Ω are large and M is small as their error in higher SNR regions is diminished.

Table 5.2: Marginal Moment Generating Functions for several fading distributions. NOTE: $\Phi(s) = \phi(s, 0)$

channel model	*pdf and the marginal mgf of signal power*
Rayleigh	$f_X(x) = \frac{1}{\Omega}\exp\left(\frac{-x}{\Omega}\right)$ $\phi_X(s,\gamma) = \frac{1}{1+s\Omega}\left[1 - e^{-\gamma(s+1/\Omega)}\right]$
Rice-K	$f_X(x) = \frac{1+K}{\Omega}e^{\left(-K-\frac{(1+K)x}{\Omega}\right)}I_0\left(2\sqrt{\frac{K(1+K)x}{\Omega}}\right)$ $\phi_X(s,\gamma) = \frac{1+K}{1+K+s\Omega}e^{-\frac{-s\Omega K}{1+K+s\Omega}}\left[1 - Q_1\left(\sqrt{\frac{2K(1+K)}{1+K+s\Omega}}, \sqrt{\frac{2(1+K+s\Omega)\gamma}{\Omega}}\right)\right]$
Nakagami-m	$f_X(x) = \left(\frac{m}{\Omega}\right)^m \frac{x^{m-1}}{\Gamma(m)}\exp\left(\frac{-mx}{\Omega}\right)$ $\phi_X(s,\gamma) = \left[\frac{m}{m+s\Omega}\right]^m\left[1 - \frac{\Gamma(m, \frac{\gamma(m+s\Omega)}{\Omega})}{\Gamma(m)}\right]$
Nakagami-q	$f_X(x) = \frac{1}{\Omega\sqrt{1-b^2}}\exp\left[\frac{-x}{(1-b^2)\Omega}\right]I_0\left[\frac{bx}{(1-b^2)\Omega}\right]$ $\phi_X(s,\gamma) = \frac{1}{\sqrt{(s\Omega+1)^2-(s\Omega b)^2}} - \frac{1}{s(1-b)^2\Omega+1}I_e\left[\frac{b}{s(1-b^2)\Omega}, \frac{x(1-b^2)\Omega}{s(1-b^2)\Omega+1}\right]$ where $-1 \le b = \frac{1-q^2}{1+q^2} \le 1; \quad 0 \le q \le \infty$
Weibull	$f_X(x) = \frac{\alpha}{2\beta^\alpha}x^{\alpha/2-1}\exp\left\{-\left(\sqrt{x}/\beta\right)^\alpha\right\}$ $\phi_X(s,\gamma)$ does not exist; MGF for integer α is [29]: $\phi_X(s) = \left(\frac{\alpha}{\eta}\right)(2\pi)^{\frac{1-\alpha}{2}}G^{1,\alpha}_{\alpha,1}\left(\eta\left(\frac{s}{\alpha}\right)^\alpha \middle\vert \begin{matrix} 1 \\ 1, 1+\frac{1}{\alpha}, \ldots, 1+\frac{\alpha-1}{\alpha}\end{matrix}\right)$ where $\eta = \beta^\alpha$

5.3 Adaptive Modulation in Slow-varying Wireless Channels

The term "adaptive" in regard to wireless radios is somewhat ambiguous as to imply a variety of schemes including variable packet length, symbol constellation size, constellation geometry, etc. In this case a method of switching between a set of modulation types, M-ary QAM or M-ary PSK, is used to achieve a specific average bit error rate (BER). Accurate knowledge of the channel's fading statistics is paramount to providing the best possible throughput while maintaining a predetermined quality of service (QoS).

For slowly-varing wireless channels, the received signal envelope is assumed to be flat for the duration of a data packet thus the modulation-switching procedure matches to the slow fading average received power. This section evaluates the performance of modulation-switching schemes relative to different fading channel assumptions.

5.3.1 System Model

The appropriate modulation levels chosen for subsequent data packets are determined on the basis of signal strength alone. In this case errors encountered within the packets are not incorporated in this analysis. In [34] Torrance and Hanzo formulated an upper bound on the bit error rates for switching adaptive M-ary QAM in a channel experiencing slowly-varying Rayleigh fading. The switching scheme assumes a time divisional duplexing (TDD) system without knowledge of errors encountered in the received data packets. As dicussed earlier, however, the Rayleigh assumption is not always an appropriate model for fading environments as it consists of only one degree of freedom, namely mean power over the packet duration. The Nakagami-m distribution is a robust model for describing fading environments, and thus is attractive for extending Torrance and Hanzo's work to incorporate various degrees of fluctuating channel conditions.

The average BER in a fading environment described by (5.5) for a single modulation type can be extended to a general expression when considering an discrete rate adaptive switching system. Given a set of M modulation types (such as M-ary PSK or M-ary QAM), a communications channel attempts to maximize data throughput while maintaining an average BER below a preset quality of service (QoS) level by selecting the best modulation scheme based on the short-time average signal power alone. Because the fading affects the signal amplitude slowly with respect to the packet duration, knowledge of the fading statistics are not required. That is, the received signal power can be considered temporarily stationary due to the large temporal correlation between samples. A narrowband upper bound BER performance of such a discrete switching scheme may therefore be computed from

$$\bar{P}_b(\Omega) = \frac{\sum_{i=1}^{N} k_i \int_{\gamma_i}^{\gamma_{i+1}} P_i(\gamma) f_\gamma(\gamma,\Omega) d\gamma}{\sum_{i=1}^{N} k_i \int_{\gamma_i}^{\gamma_{i+1}} f_\gamma(\gamma,\Omega) d\gamma} \tag{5.10}$$

where Ω is the average signal power, $k_i = \log_2(M_i)$ bits per symbol for the modulation type, γ_i is the threshold SNR, and $P_i(\gamma)$ is the BER distribution for the i^{th} modulation type under an AWGN channel. Note that the denominator is the average spectral efficiency, $\bar{\eta}(\Omega)$. For most modulation schemes, P_M is often a sum of complimentary error functions (erfc), thus, depending on the distribution, a closed-form analytical expression for $\bar{P}_M(\Omega)$ cannot be derived. For a Nakagami channel this expression can actually recude to a sum of finite bounded integrals, however a simpler solution which does not rely on the cumbersome task of numerical integration is desired. Employing the linear BER approximation from section 5.2.1 however, (5.10) reduces to

$$\bar{P}_b(\Omega) \approx \frac{\sum_{i=1}^{N} a_i k_i \left[\phi(b_{i+1},\gamma_{i+1}) - \phi(b_i,\gamma_i)\right]}{\sum_{i=1}^{N} k_i \left[\phi(0,\gamma_{i+1}) - \phi(0,\gamma_i)\right]} \tag{5.11}$$

where $\phi(s,x) = \int_x^\infty f_x(x) e^{-sx} dx$ is the marginal moment generating function (mMGF) of

signal power for the fading distribution. Table 5.2 gives the mMGF for several fading distributions. If the second-order BER approximation given by (5.4) were used, the average adaptive BER would be

$$\bar{P}_b(\Omega) \approx \frac{\sum_{i=1}^{N} k_i \left\{ a_i \left[\phi(b_{i+1}, \gamma_{i+1}) - \phi(b_i, \gamma_i) \right] + c_i \left[\phi(2b_{i+1}, \gamma_{i+1}) - \phi(2b_i, \gamma_i) \right] \right\}}{\sum_{i=1}^{N} k_i (a_i + c_i) \left[\phi(0, \gamma_{i+1}) - \phi(0, \gamma_i) \right]} \tag{5.12}$$

The average spectral efficiency is calculated as

$$\bar{\eta}(\Omega) = \sum_{i=1}^{N} k_i \int_{\gamma_i}^{\gamma_{i+1}} f\gamma(\gamma, \Omega) d\gamma \tag{5.13}$$

When using a Nakagami model, (5.13) collapses to

$$\bar{\eta}(\Omega) = \frac{1}{\Gamma(m)} \sum_{i=1}^{N} k_i \left[\Gamma(\frac{m\gamma_{i+1}}{\Omega}, m) - \Gamma(\frac{m\gamma_i}{\Omega}, m) \right] \tag{5.14}$$

where $\Gamma(a, x)$ is the lower incomplete Gamma function (see Appendix A). Notice that (5.14) is an exact solution.

5.3.2 Results and Discussions

Figure 5.3 shows the BER performance of a Nakagami-m channel where numerical integration and the two approximations, (5.11) and (5.12), were used to solve (5.12) to approximate the upper bound of BPSK, QPSK, 16-, and 64-QAM. The adaptive channel performance was determined by assuming perfect coherent receiver detection with switching levels 0, 8, 14, and 20dB between no transmission (off) and the modulation schemes. The switching levels were chosen in accordance with Torrance and Hanzo's work, on the basis that the mean BERs for the modulation types are approximately 1% in an uncoded AWGN channel. Figure 5.3(a) matches closely with [35, Fig. 1]. Furthermore, the approximations are accurate over a broad range of Ω and m while preserving a considerably lower computational complexity. The approximations fit well to the numerical integral results particularly when m and Ω are large.

As expected, as m approaches infinity, the BER curves approach those of the AWGN channel and the adaptive modulation curve fits the AWGN BER contours, switching modulation schemes at approximately the QoS threshold. Indeed for Nakagami, $\lim_{m\to\infty} \phi(s, 0) = e^{-s\Omega}$ which is exactly the 1^{st}-order BER approximation assumed in an AWGN channel. It is apparent from Figure 5.4 that for situations where the channel's fading is better than Rayleigh ($m > 1$) the throughput improves.

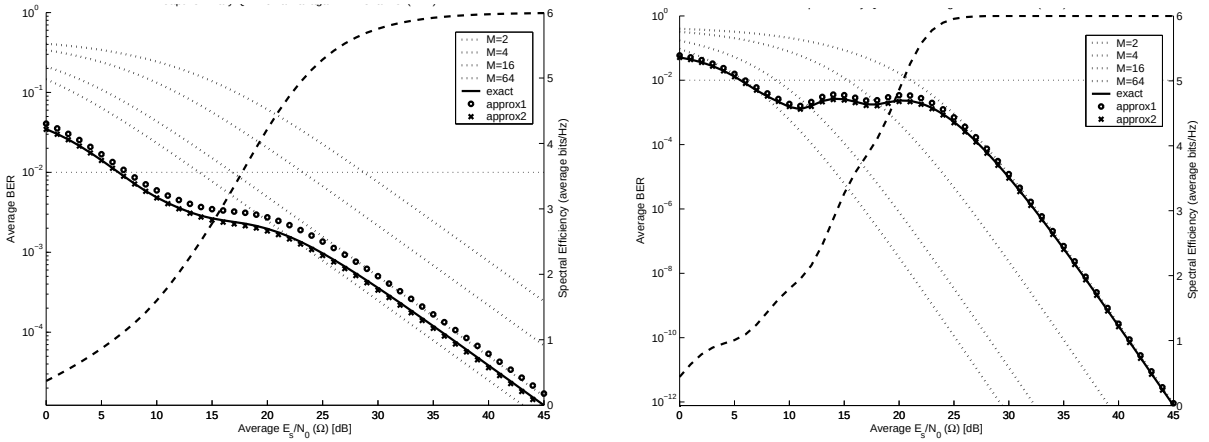

(a) $m = 1$ (Rayleigh)

(b) $m = 5$

Figure 5.3: Exact BER performances of BPSK, QPSK, 16-, and 64-QAM adaptive modulation under a Nakagami-m faded channel as well as two approximations for adaptive modulation BERs and average spectral efficiency. Switching levels are 0, 8, 14, and 20dB chosen for a maximum BER performance of 10^{-2} in an AWGN channel.

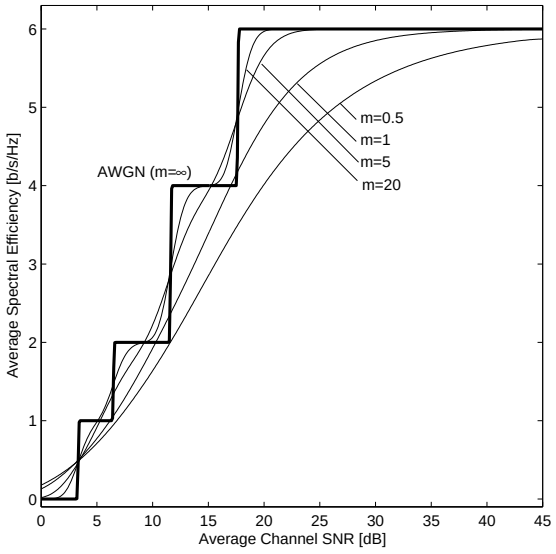

Figure 5.4: Throughput performance of adaptive modulation on Nakagami-m faded channels using 2-, 4-, 16-, and 64-QAM with switching levels 0, 8, 14, and 20dB (optimum in AWGN channel)

5.3.3 Optimal switching levels

In [35] Torrance and Hanzo discussed an optimal power-level switching algorithm to maximize throughput while preserving the preset QoS. Obviously these levels will change with the fading profile, however empirical evidence suggests that m is not a considerable factor (see Fig. 5.5). Observing that the optimized switching levels for M-ary QAM do not significantly change with m, the initial AWGN threshold levels could be used.

The tradeoff for improved spectral efficiency is a higher bit error rate. For a given target QoS and throughput, optimal switching thresholds can be determined by the method proposed in [35], but can be generalized to different fading distributions, rather than just Rayleigh. Devising a similar approach to [35], the total cost for

$$\text{total cost} = \sum_{i=0}^{N} f^c_{BPS}(\Omega_i) + f^c_{BER}(\Omega_i) \tag{5.15}$$

where f^c_{BPS} and f^c_{BER} are the cost functions for spectral efficiency and bit error rate respectively, defined below:

$$f^c_{BER}(\Omega) = \begin{cases} 10\log_{10}\left[\frac{\bar{P}_M(\Omega)}{\bar{P}_d(\Omega)}\right] & \bar{P}_M(\Omega) > \bar{P}_d(\Omega) \\ 0 & \text{else} \end{cases} \tag{5.16}$$

$$f^c_{BPS}(\Omega) = \begin{cases} \bar{\eta}_d(\Omega) - \bar{\eta}_M(\Omega) & \bar{\eta}_d(\Omega) > \bar{\eta}_M(\Omega) \\ 0 & \text{else} \end{cases} \tag{5.17}$$

where $\bar{P}_M(\Omega)$, $\bar{P}_d(\Omega)$, $\bar{\eta}_M(\Omega)$, and $\bar{\eta}_d(\Omega)$ are the total average BER of all modulation types (given a specific fading distribution) given by (5.10), the desired average BER, the average spectral efficiency given by (5.13), and the desired spectral efficiency, respectively.

Optimum switching levels for M-ary QAM in a Nakagami-m channel were calculated iteratively using the cost function described above on average SNR ranging from 0 to 50dB for several values of m. Two target BERs of 10^{-2} ("speech") and 10^{-4} ("data") were analyzed with respective desired spectral efficiencies ($\bar{\eta}_d$) of 4 and 3 bits per second. The results can be seen in Figure 5.5. The results match closely with those of [35] discussed for Rice-K channels; namely that as m increases the BPS performance is more undulating, approaching that of an AWGN channel (see Figure 5.4).

5.4 Adaptive Modulation in Outdoor, Fast Fading Environments

Adaptive modulation exploits the BER characteristics of different modulation schemes in order to mitigate the effects narrowband multipath channels have on wireless radio links.

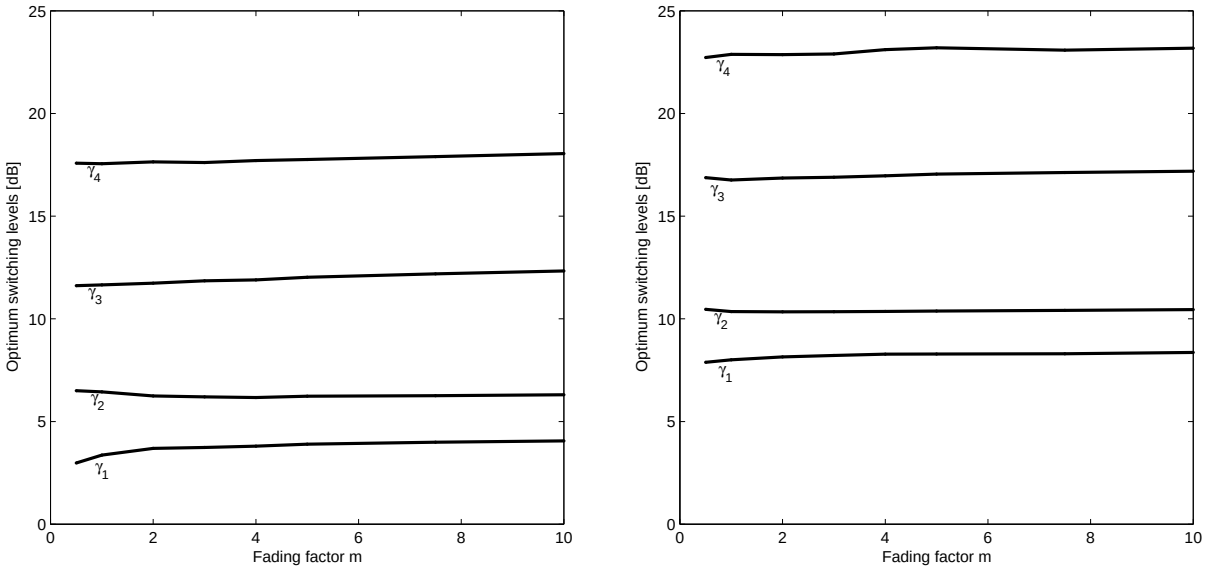

(a) QoS $= 10^{-2}$ (b) QoS $= 10^{-4}$

Figure 5.5: Optimized switching levels for M-ary QAM in a Nakagami-m faded channel calculated for SNR ranging from 0 to 50dB. Switching levels are between off (no transmission), BPSK, QPSK, 16- and 64-QAM, respectively.

Fast fading is often an issue in outdoor environments where the power level fluctuates quickly within the duration of a single packet. As discussed in Section 5.3 for slow fading, the channel is assumed to be pseudo-stationary for the duration of the packet, thus only the short-term average power is needed in order to determine an appropriate modulation scheme for a desired average BER. However, in certain environments where the received power fluctuates quickly, the channel can experience several deep fades within the duration of a single data packet. Accurate knowledge of the fading severity is therefore required to meet a desired QoS while maximizing throughput.

5.4.1 System Model

In addition to fast fading, there is also a slower variation in the received mean power. Referred to as shadowing, this phenomenon usually occurs as a result of obstacle obstruction and large scale path loss, largely dependent upon local terrain and civil structures. Empirical data [1, 37] demonstrate that the log-normal distribution is a good model for describing outdoor shadowing trends. The log-normal distribution of signal power (Gaussian distributed if measured in dB) is defined as

$$f_\Omega(\Omega;\mu,\sigma) = \frac{1}{\xi\Omega\sqrt{2\pi\sigma^2}} \exp\left\{-\frac{(\ln(\Omega)-\mu)^2}{\xi 2\sigma^2}\right\} \tag{5.18}$$

where μ is the long-term average signal power in dB, σ is the standard deviation of the signal power in dB, and $\xi = \ln 10/10$. Typical values of σ are under 6dB for light and 9dB or more for heavy shadowing. The log-normal power is used to generate the average signal power for the fast-fading component. Because the random variables used for the shadowing and fast-fading components are assumed independent, they can be generated independently and combined later. In practice this may not be the case; for instance, if the receiver is shadowed by a structure, its line-of-sight component is significantly reduced, thus increasing the possibility of more severe fast fading. Generating correlated non-stationary random variables (with fluctuating fading profiles), however, is difficult, and thus presents some limitations to this model where the envelope of signal power over time can be modeled as a non-stationary stochastic process in which the average power fluctuates, but the fading profile (i.e. the Rice K-factor) is a constant

5.4.2 Doppler filter

Statistical measurements suggest samples will exhibit correlation in accordance with the user's Doppler frequency. For the Rice-K distribution, this is modeled as a single LoS component arriving at a specific angle of arrival to the user's velocity. This signal arrives amidst an array of incoming scattered components whose angle of arrival is distributed about

the receiver. If this distribution is uniform, the resulting autocorrelation function is the well-known Clarke-Jakes model, expressed as $r_h(\tau) = J_0(2\pi f_d t)$ [20] whose power spectral density (PSD) is

$$\Phi(f) = \frac{1.5}{\sqrt{(K+1)\pi f_d \left[1 - \left(\frac{f}{f_d}\right)^2\right]}} + 1.5\left(\frac{K}{K+1}\right)\delta\left(f_d\cos(\theta)\right) \tag{5.19}$$

where $f_d = f_c(\nu/c)$ is the maximum doppler frequency, f_c is the carrier frequency, ν is the user velocity, c is the speed of light, K is the fading factor, and θ is the AoA of the LoS signal.

A statistical measurement of the log-normal shadowing autocorrelation function has been verified experimentally [1] to be

$$\rho(t) = e^{-0.0101 f_d \lambda_c t} \tag{5.20}$$

which has an equivalent power spectral density

$$\Phi(f) = \frac{1}{0.0101 f_d \lambda_c + j2\pi f} \tag{5.21}$$

where λ_c is the carrier wavelength. A plot of the PSDs of the doppler filters for both Rice-K fast fading and log-normal shadowing can be seen in Figure 5.6. Notice that the shape of the log-normal shadowing filter removes high frequency components and passes only very low frequencies. This implies a slowly-varying channel, as one would expect. Conversely, the Rice-K doppler filter accepts frequencies near f_d and rejects others which implies the channel experiences temporal periodic fades related to the user's speed.

5.4.3 Simulation

Sequences of received power were generated using the method in Figure 5.7 with correlated log-normal and Rice-K random variables, with data blocks 256 symbols each. M-ary QAM was the assumed modulation scheme, the constellation size determined by the average block power and fading statistic. Intuitively, the length of the block will affect the performance. In typical systems there is some overhead to each block, thus the actual throughput will be improved with longer block lengths. Additionally channel estimators demonstrate lower error with longer sequences. However, if the block is too long, the channel changes quickly in relation; the average power is assumed to be constant over the packet duration, thus performance will suffer for blocks that are too long.

5.4.4 Results and Conclusions

The approximations to BER from (5.1) and especially (5.1) when applied to Nakagami-m fading environments provide simple and uniquely invertible expressions for performance in

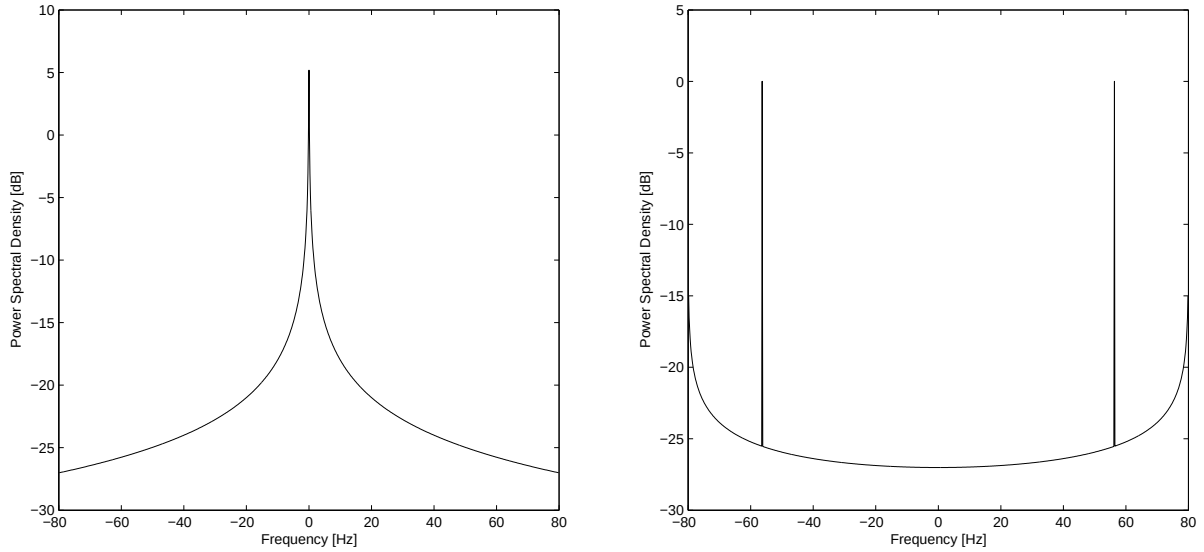

(a) Log-normal (b) Rice-K

Figure 5.6: Doppler filter power spectral density. Maximum doppler frequency 80Hz, $K = 2$, AoA $= 45°$.

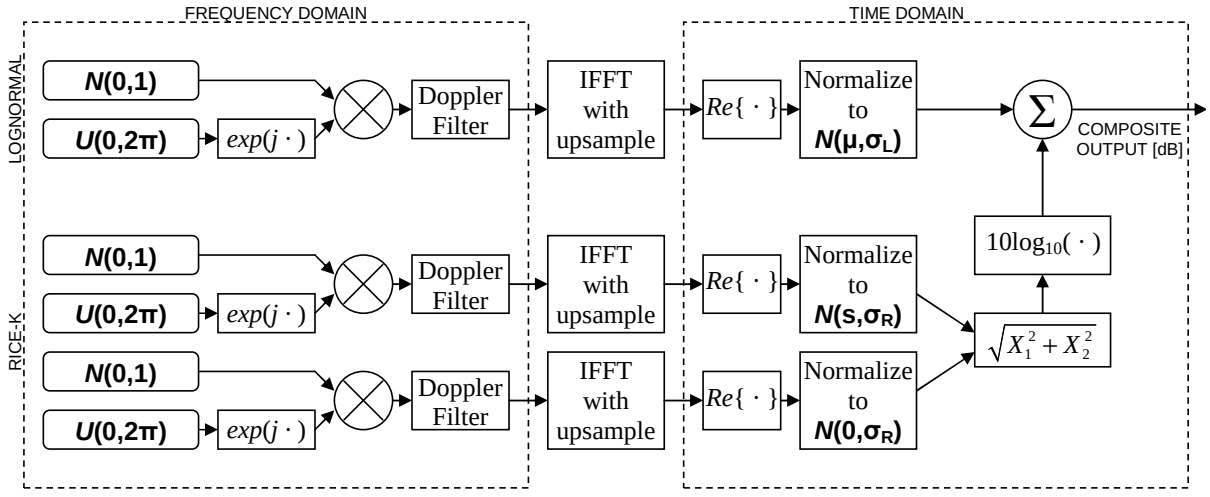

Figure 5.7: Diagram for generating composite log-normal/Rice-K sequences with inputs σ_L (dB), μ (dB), K, AoA, and f_d. Note that a Rice RV can be generated from two Gaussian RVs: $X_1 \sim N(0, \sigma_R)$, and $X_2 \sim N(s, \sigma_R)$ where $s^2 = \frac{\Omega K}{K+1}$ and $\sigma_R^2 = \frac{\Omega}{2(K+1)}$. In this case the mean power for the Rice-K distribution is 0dB, so Ω is set equal to 1.

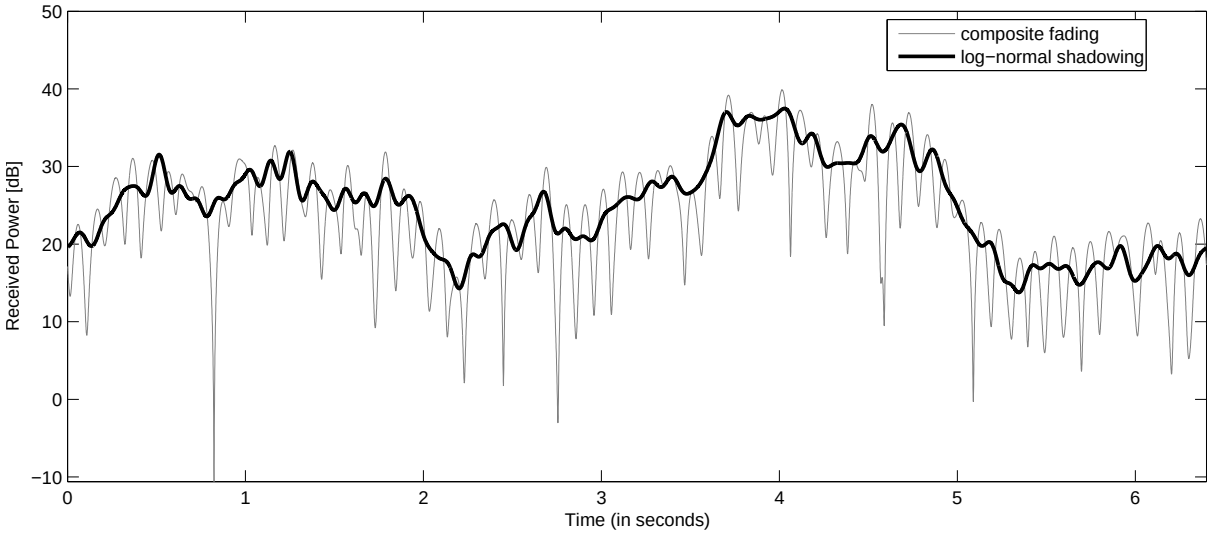

(a) Received power

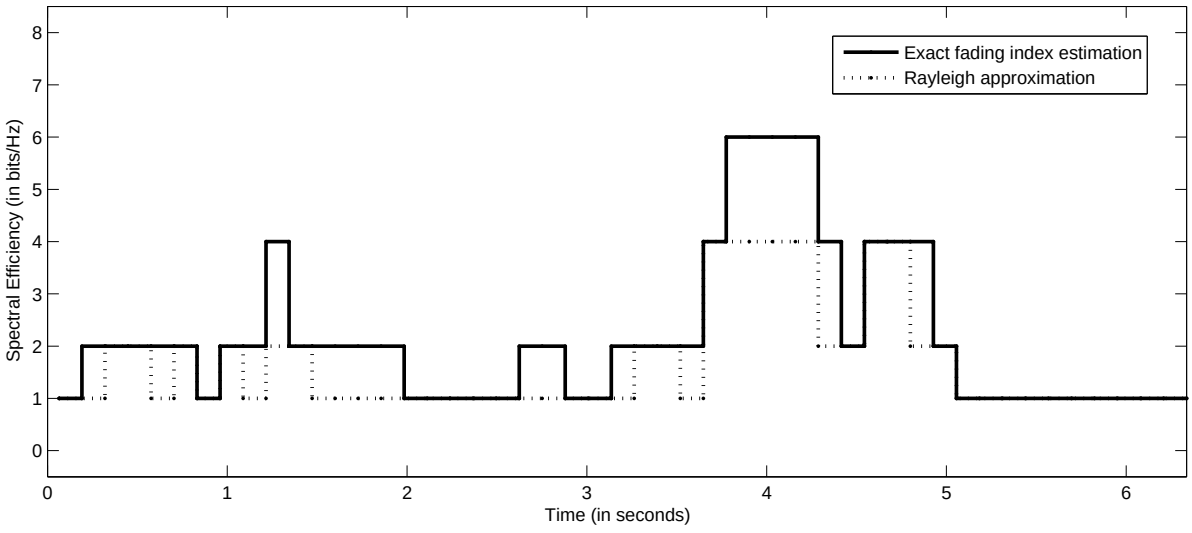

(b) Average spectral efficiency

Figure 5.8: "Channel 1," Simulated sequence of 50 packets of 256 symbols each. Channel parameters are: $f_d = 10$ Hz, $\sigma = 6$dB, $\mu = 25$dB, $K = 2$

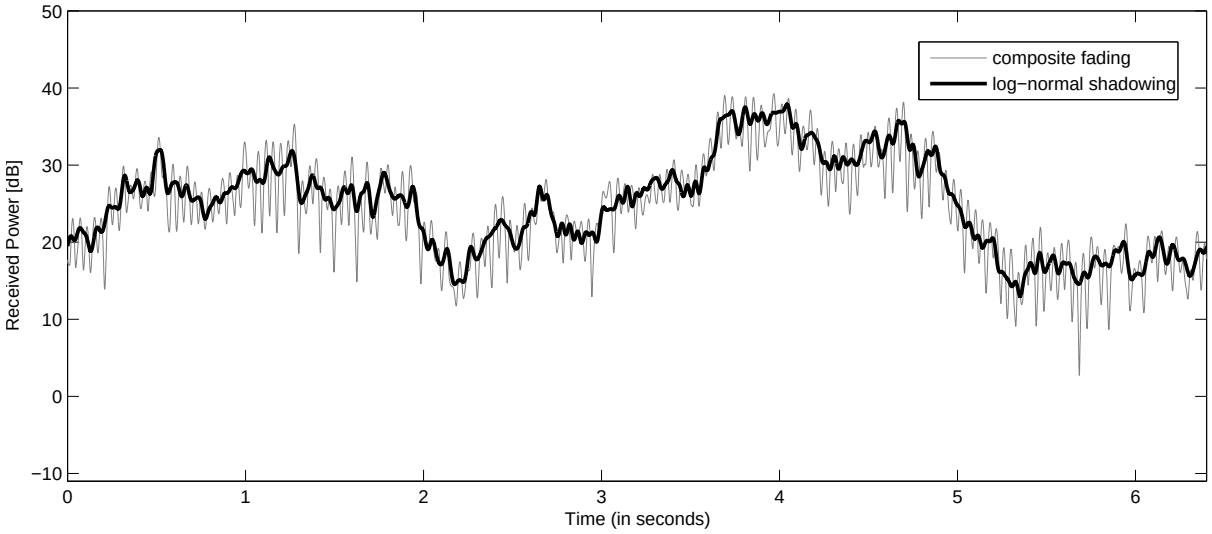

(a) Received power

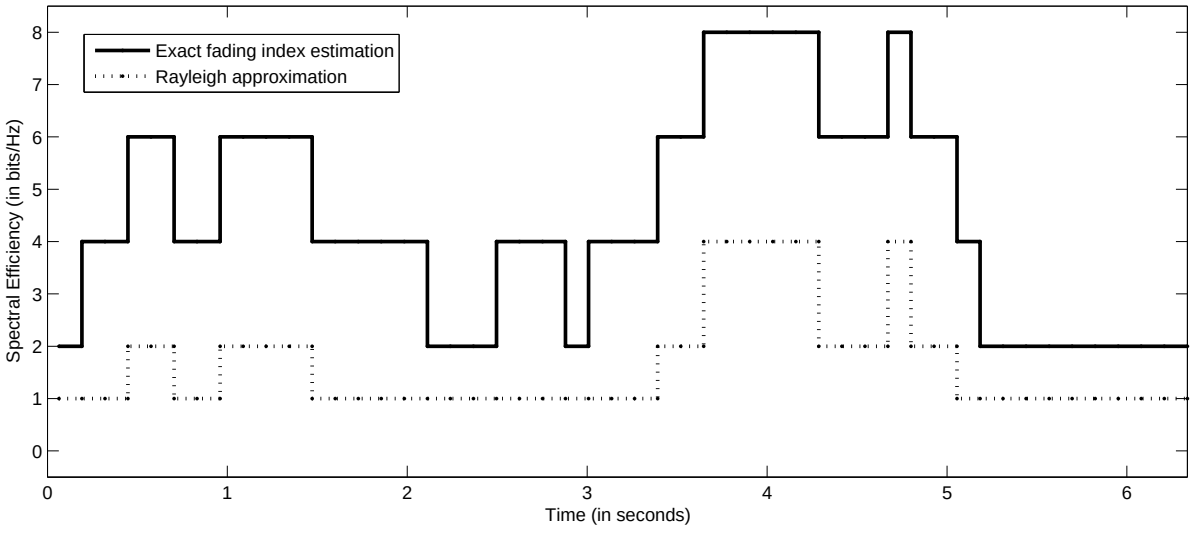

(b) Average spectral efficiency

Figure 5.9: "Channel 2," Simulated sequence of 50 packets of 256 symbols each. Channel parameters are: $f_d = 25$ Hz, $\sigma = 6$dB, $\mu = 25$dB, $K = 6$

channels with a particular average signal. Their usefulness in adaptive systems is apparent, and can be seen in Figures 5.3 and 5.4.

Furthermore, the results of two simulated channels can be seen in Figures 5.8 and 5.9. Although the channel model is assumed to be ideal (where perfect knowledge of the fading parameters are known) the benefits of channel probing over the Rayleigh assumption are transparent, especially in Figure 5.9 (K=6) where the average spectral efficiency is consistently greater than under the Rayleigh assumption.

At first glance it may seem that increasing the packet size can arbitrarily improve throughput performance, as the estimators generally improve with larger sample sizes. However this assumption does not necessarily hold for two basic reasons:

1. The channel's mean power is constantly shifting, thus assuming a parent distribution with a constant mean power is inherently flawed. For smaller sample sizes, however, this assumption works well, but at the cost of estimator performance.

2. Because the channel is changing, an estimation of the fading characteristics at one time does not necessarily reflect the channel conditions at another. Using a one packet on which to make a decision for the very next packet assumes the channel has not significantly changed over the packet delay, which is not necessarily true. Using longer packets increases this delay and thus is the source for error.

Figures 5.10, 5.11, and 5.12, demonstrate the effect of packet length on throughput. For the TDD system proposed in this section, the channel's fading parameters are estimated on the first half of the packet (assuming a Nakagami-m distribution) and a decision for which modulation scheme to be used for the next packet is made based on these statistics, using (5.8). If the actual BER for that packet (based on the true channel statistics) is greater than the desired QoS, the entire packet is assumed to be in error and the spectral efficiency is zero. The same channel was used for three TDD systems with different packet lengths; 256, 512, and 1024 symbols per packet. The average throughput improvement the Nakagami-m channel has over the Rayleigh assumption for a packet length of 256 symbols (basing its estimates for m and Ω on the first 128 samples) is a marginal 1.71 bps better, doubling the packet length to 512 symbols improves its performance even more to 2.10 bps. Doubling the packet length again, however, reduces this to a 1.88 bps improvement over Rayleigh. Even though the packet error rate for the third case has not degraded, the cost of losing a single packet may be higher.

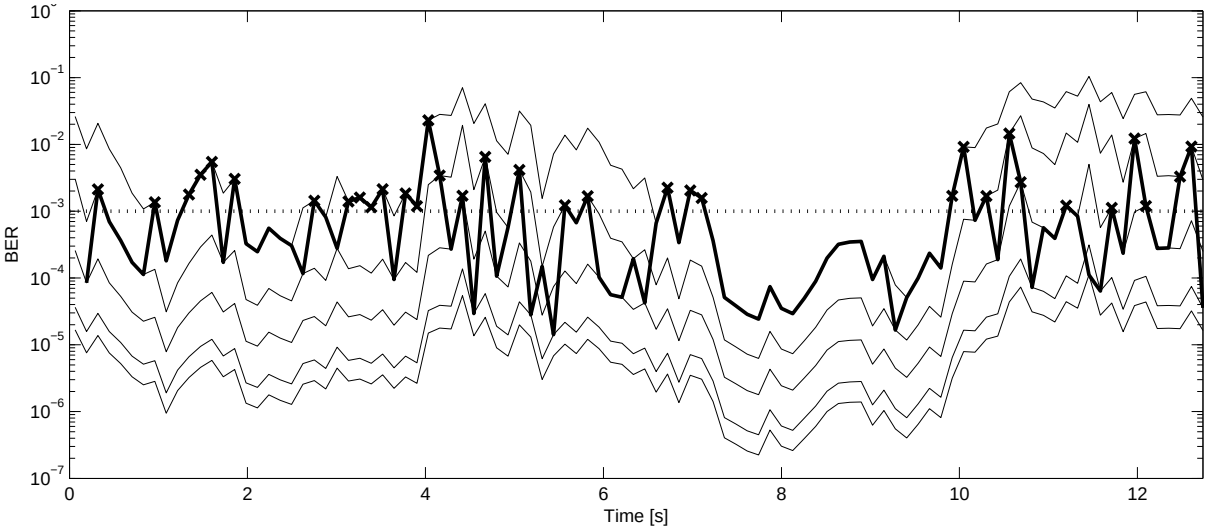

(a) BER (34/100 packets in error)

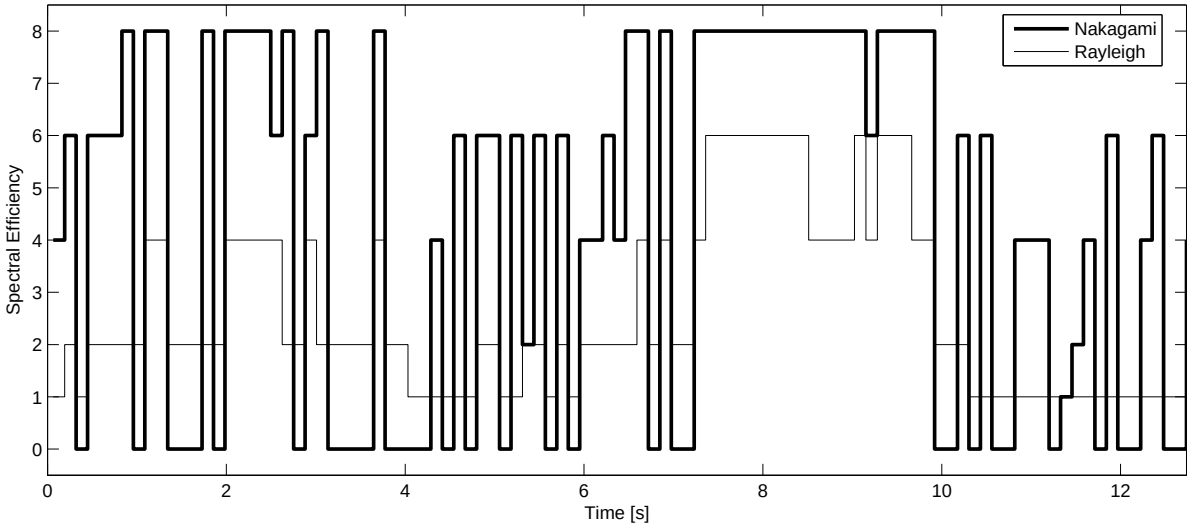

(b) Average spectral efficiency (average improvement of Nakagami over Rayleigh: 1.71 bps)

Figure 5.10: Simulated sequence of 100 packets of 256 symbols each. Channel parameters are: $f_d = 25$ Hz, $\sigma = 6$dB, $\mu = 25$dB, $K = 6$.

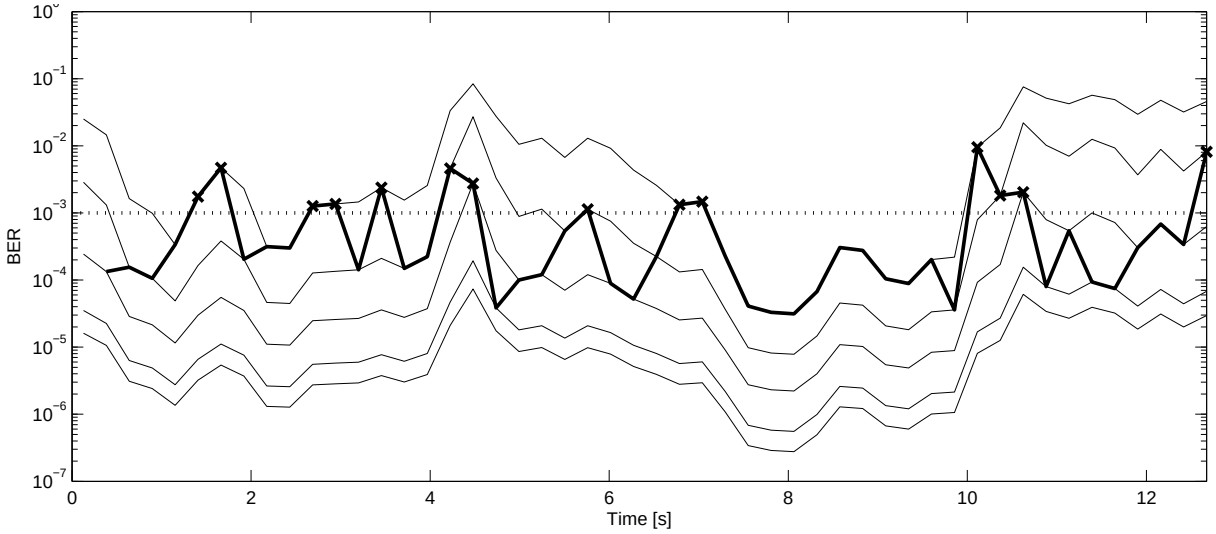

(a) BER (14/50 packets in error)

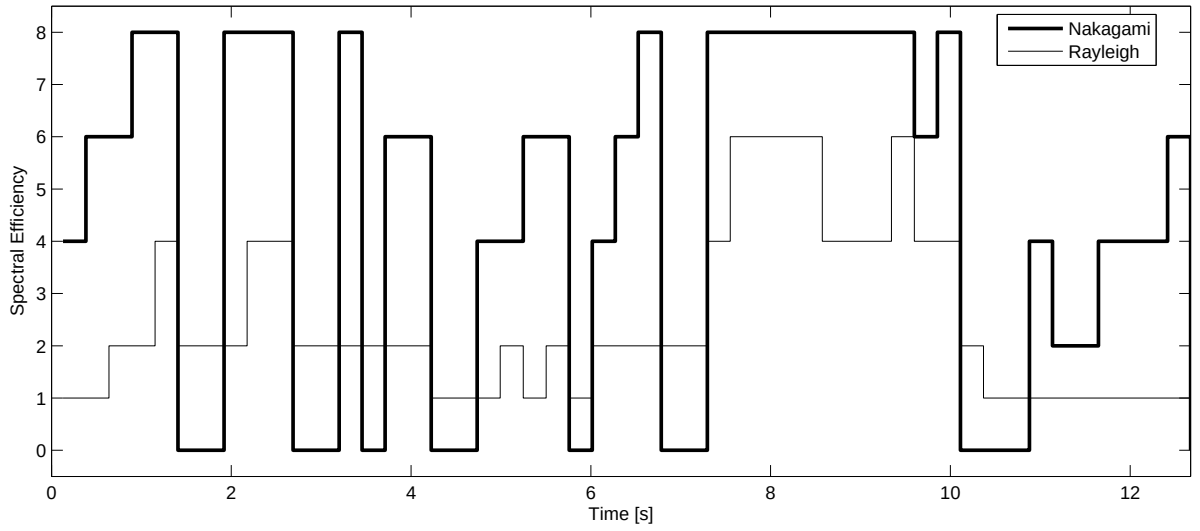

(b) Average spectral efficiency (average improvement of Nakagami over Rayleigh: 2.10 bps)

Figure 5.11: Simulated sequence of 50 packets of 512 symbols each. Channel parameters are: $f_d = 25$ Hz, $\sigma = 6$dB, $\mu = 25$dB, $K = 6$.

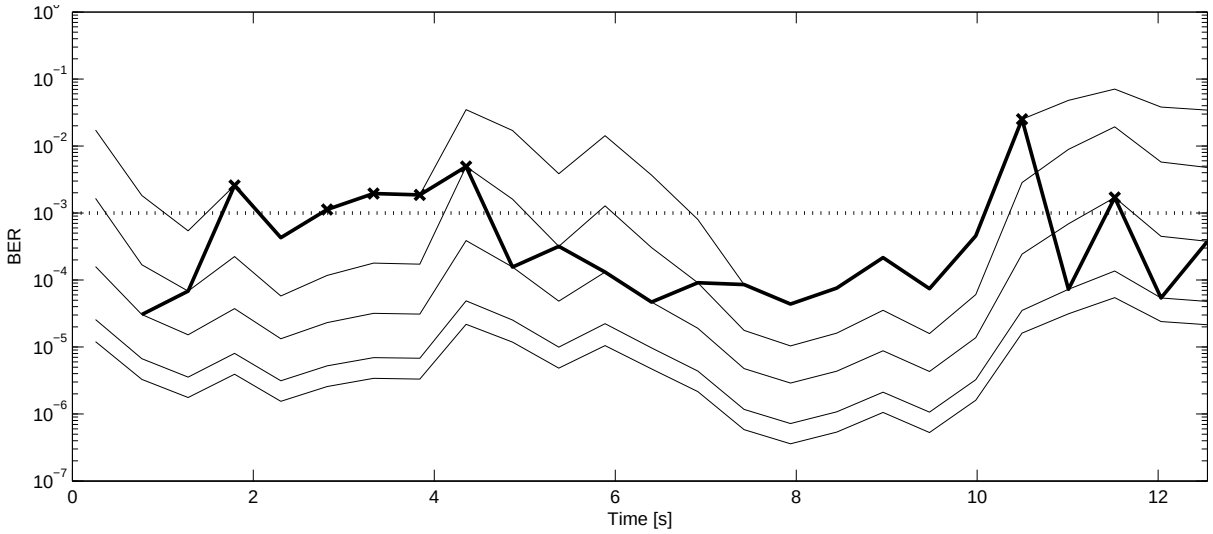

(a) BER (7/25 packets in error)

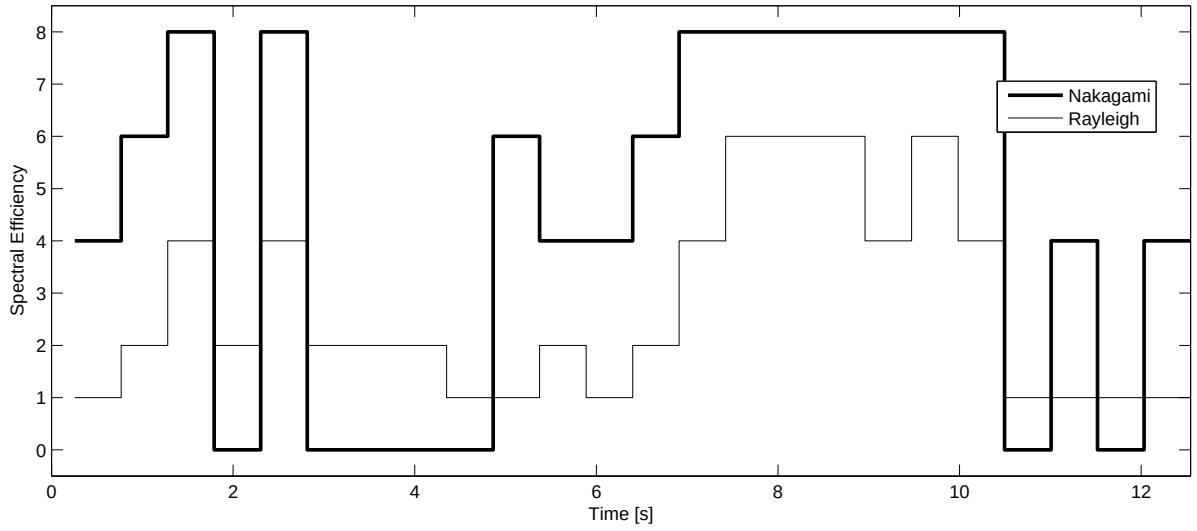

(b) Average spectral efficiency (average improvement of Nakagami over Rayleigh: 1.88 bps)

Figure 5.12: Simulated sequence of 25 packets of 1024 symbols each. Channel parameters are: $f_d = 25$ Hz, $\sigma = 6$dB, $\mu = 25$dB, $K = 6$.

Chapter 6

Concluding Remarks

Mathematical modeling tools are powerful methods for characterizing fading channels in wireless communications systems. Statistical models, such as Nakagami-m, Rice-K, and Weibull can be used to describe distributions of received signal strength subject fading (due to path loss and multi-path reception at the receiver) on narrowband systems. Accurate and efficient estimation of the channel's fading severity is paramount for the success of adaptive radios, thus parameters inherent to these mathematical distributions which describe channel fading profile need to be estimated.

The results of the estimation techniques described in the work demonstrate that polynomial approximation and asymptotic approximation techniques provide simple closed-form solutions and perform similarly to iterative solutions while preserving a lower computational complexity and run time. By using approximations iterative solutions to transcendental equations in the estimators can be circumvented with appropriate results. Furthermore, in the case of moment estimation, previous work on the subject has resorted to using higher-order moments in order to solve for the fading parameters in closed form, however the approximation methods described herein can be applied to situations where otherwise only iterative solutions are available. Empirical evidence suggests that these estimators, based on lower-order moments, are particularly robust and resistant to outliers in the sample set. The optimized coefficients for the approximating solutions have been calculated (a task performed offline) and tabulated.

In addition, unified expressions for bit error rates (BER) and average spectral efficiencies for adaptive switching modulation schemes are provided which characterize upper bound performances on narrowband wireless systems exhibiting fading. Adaptive systems exploit the BER characteristics of different modulation schemes in order to mitigate the effects of slow fading and shadowing apparent in short-time average received signal power, however unless accurate knowledge of the channel's fading parameters are known, the system perfor-

mance in fast-fading environments degrades significantly. Often for this reason the Rayleigh fading assumption is made, which is often pessimistic and throughput of the system suffers as a result, ergo the impact fading has on such systems is directly dependent upon its severity. Accurate knowledge of the channel's fading statistics provide significant throughput improvements on systems which attempt to adapt to shifting wireless link conditions.

Bibliography

[1] S. Hara, A. Ogino, M. Araki, M. Okada, and N. Morinaga, "Throughput performance of SAW-ARQ protocol with adaptive packet length in mobile packet data transmission," *IEEE Transactions on Vehicular Technology*, vol. 45, no. 3, pp. 561–9, August 1996.

[2] C. E. Shannon, "A mathematical theory of communication," *Bell Systems Technical Journal*, vol. 27, pp. 623–56, October 1948.

[3] W. R. Braun and U. Dersch, "A physical mobile radio channel model," *IEEE Transactions on Vehicular Technology*, vol. 40, pp. 472–482, February 1991.

[4] M. K. Simon and M. S. Alouini, "A unified approach to the performance analysis of digital communication over generalized fading channels," *Proceedings of the IEEE*, vol. 86, no. 9, September 1998.

[5] G. L. Turin, "Introduction to spread-spectrum anti-multipath techniques and their applications to urban digital radio," *Proc. IEEE*, vol. 68, pp. 328–53, March 1980.

[6] H. Suzuki, "A statistical model for urban radio propagation," *IEEE Trans. on Comm.*, vol. COM-25, pp. 673–80, July 1977.

[7] J. K. Cavers, "Optimized use of diversity modes in transmitter diversity systems," in *Vehicular Technology Conference*, April 1999, pp. 1768–1773.

[8] Y. C. Ko and M. Alouini, "Estimation of Nakagami-m fading channel parameters with application to optimized transmitter diversity systems," *IEEE Transactions on Wireless Communications*, vol. 2, no. 2, pp. 250–259, March 2003.

[9] V. E. S. Catreux and R. Heath, "Adaptive modulation and MIMO coding for broadband wireless data networks," *IEEE Communications Magazine*, pp. 108–115, June 2002.

[10] A. Abdi and M. Kaveh, "Performance comparison of three different estimators for the Nakagami m parameter using Monte Carlo simulation," *IEEE Communications Letters*, vol. 4, pp. 119–121, April 2000.

[11] J. Cheng and N. Beaulieu, "Maximum-likelihood based estimation of the Nakagami-m parameter," *IEEE Communications Letters*, vol. 5, pp. 101–103, March 2001.

[12] ——, "Generalized moment estimators for the Nakagami fading parameters," *IEEE Communications Letters*, vol. 6, pp. 144–146, April 2002.

[13] Q. T. Zhang, "A note on the estimation of Nakagami-m fading parameter," *IEEE Communications Letters*, vol. 6, pp. 237–238, June 2002.

[14] A. Papoulis and S. U. Pillai, *Probability, Random Variables and Stochastic Processes*, 4th ed. Boston: McGraw-Hill, 2002.

[15] Y. L. Luke, *Mathematical Functions and Their Approximations*. Academic Press, 1975.

[16] M. Spiegel and J. Leu, *Schaum's Outline Series: Mathematical Handbook of Formulas and Tables*, 2nd ed. New York: McGraw-Hill, 1999.

[17] L. J. Greenstein, D. G. Michelson, and V. Erceg, "Moment-method estimation of the Rice K-Factor," *IEEE Communications Letters*, vol. 3, no. 6, June 1999.

[18] G. Azemi, B. Senadji, and B. Boashash, "Ricean K-factor estimation in mobile communications systems," *IEEE Communications Letters*, vol. 8, no. 10, October 2004.

[19] A. Abdi, C. Tepedelenlioğlu, M. Kaveh, and G. Giannakis, "On the estimation of the parameter for the Rice fading distribution," *IEEE Communications Letters*, vol. 5, no. 3, March 2001.

[20] C. Tepedelenlioğlu, A. Abdi, and G. Giannakis, "The Ricean K factor: Estimation and performance analysis," *IEEE Transactions on Wireless Communications*, vol. 4, no. 2, July 2003.

[21] H. Hashemi, "The indoor radio propagation channel," *Proceedings of the IEEE*, vol. 81, no. 7, pp. 943–68, 1993.

[22] G. Tzeremes and C. G. Christodoulou, "Use of Weibull distribution for describing outdoor multipath fading," *Antennas and Propagation Society International Symposium*, vol. 1, pp. 232–5, June 2002.

[23] N. S. Adawi, H. L. Bertoni, J. R. Child, *et al.*, "Coverage prediction for mobile radio systems operating in the 800/900 MHz frequency range," *IEEE Vehicular Technology Society Committee on Radio Propagation*, vol. 37, no. 1, February 1988.

[24] P. Fannin and A. Molina, "Analysis of mobile radio channel sounding measurements in inner city Dublin at 1.808 GHz," *IEE Proceedings on Communications*, vol. 143, pp. 311–6, October 1996.

[25] N. Shepherd, "Radio wave loss deviation and shadow loss at 900 MHz," *IEEE Transactions on Vehicular Technology*, vol. 26, 1997.

[26] K. Pahlavan and A. Levesque, *Wireless Information Networks*. NY: John Wiley & Sons, 1995, section 4.6.2.

[27] Alouini and Simon, "Performance of generalized selection combining over Weibull fading channels," in *Vehicular Technology Conference*, vol. 3, October 2001, pp. 1735–9.

[28] N. C. Sagias, D. A. Zogas, G. K. Karagiannidis, and G. S. Tombras, "Performance analysis of switched diversity receivers in Weibull fading," *Electronics Letters*, vol. 39, pp. 1472–4, October 2003.

[29] T. J. Cheng and N. Beaulieu, "Performance of digital linear modulations on Weibull slow-fading channels," *IEEE Transactions on Communications*, vol. 52, pp. 1265–8, August 2004.

[30] E. Gourdin, P. Hansen, and B. Jaumard, "Finding maximum likelihood estimators for the three-parameter Weibull distribution," *Journal of Global Optimization*, no. 5, pp. 373–97, 1994.

[31] U. Schmid, "Percentile estimators for the three-parameter Weibull distribution for use when all parameters are unknown," *Commun. Statist.–Theory Meth.*, vol. 26, no. 3, pp. 765–85, 1997.

[32] G. W. Cran, "Moment estimators for the 3-parameter Weibull distribution," *IEEE Transactions on Reliability*, vol. 37, no. 4, October 1988.

[33] J. Jacquelin, "A reliable algorithm for the exact median rank function," *IEEE Transactions on Electrical Insulation*, vol. 28, no. 2, pp. 168–71, April 1993.

[34] J. Torrance and L. Hanzo, "Upper bound performance of adaptive modulation in a slow Rayleigh fading channel," *Electronics Letters*, vol. 32, no. 8, pp. 718–9, April 1996.

[35] ——, "Optimisation of switching levels for adaptive modulation in slow Rayleigh fading," *Electronics Letters*, vol. 32, no. 13, pp. 1167–9, June 1996.

[36] S. J. Howard and K. Pahlavan, "Doppler spread measurements of indoor radio channel," *Electronic Letters*, vol. 26, no. 2, January 1990.

[37] W. C. Jakes, *Microwave Mobile Communications*. New York: Wiley, 1974.

[38] I. S. Gradshteyn and I. M. Ryzhik, *Table of Integrals, Series and Products*, 6th ed. New York: Academic, 2000.

Appendix A

Special Functions

This appendix lists several uncommon functions and equations relevant to the work.

Q-Function [15]

$$Q(x) = \frac{1}{\sqrt{2\pi}} \int_x^\infty e^{-\tau^2/2} d\tau \tag{A.1}$$

Complementary error function [16, p. 200]

$$\operatorname{erfc}(x) = \frac{2}{\sqrt{\pi}} \int_x^\infty e^{-\tau^2} d\tau \tag{A.2}$$

Gamma function [16, p. 146]

$$\Gamma(a) = \int_0^\infty t^{a-1} e^{-t} dt \tag{A.3}$$

Incomplete Gamma function [15]

$$\gamma(a, x) = \int_0^x t^{a-1} e^{-t} dt \tag{A.4}$$

Pochhammer symbol [15]

$$(x)_n = \frac{\Gamma(x+n)}{\Gamma(x)} \tag{A.5}$$

Generalized Bernoulli polynomial [15]

$$B_k^{(x)}(y) \tag{A.6}$$

Marcum Q-function, M^{th} order [15]

$$Q_M(\alpha,\beta) = \frac{1}{\alpha^{M-1}} \int_{\beta}^{\infty} x^M \exp\left[-\left(\frac{x^2+\alpha^2}{2}\right)\right] I_{M-1}(\alpha x) dx \tag{A.7}$$

Modified Bessel function (expansion) [15]

$$I_\nu(z) = \left(\frac{z}{2}\right)^\nu \sum_{k=0}^{\infty} \frac{\left(z^2/4\right)^k}{k!\Gamma(\nu+k+1)} \tag{A.8}$$

Confluent Hypergeometric function [15]

$${}_1F_1(a;b;x) = \frac{\Gamma(b)}{\Gamma(b-a)\Gamma(a)} \int_0^1 e^{xt} t^{a-1} (1-t)^{b-a-1} dt \tag{A.9}$$

Rice's I_e function [15]

$$I_e(\tfrac{v}{u},u) = \frac{u}{w}\left[Q_1(\sqrt{u+w},\sqrt{u-w}) - Q_1(\sqrt{u-w},\sqrt{u+w})\right];\ w = \sqrt{u^2-v^2} \tag{A.10}$$

Meijer's G function [38, Eq. (9.301)]

$$G_{p,q}^{m,n}(\ \cdot\ ) \tag{A.11}$$

Vita

Joseph was born on a sunny day in Albuquerque, NM on July 22, 1980. He received his B.S. degree in Electrical Engineering from the University of Kentucky in 2002 and subsequently joined the Bradley Department of Electrical and Computer Engineering at Virginia Polytechnic Institute and State University beginning in the Fall of 2002.

After spending one year as a Graduate Teaching Assistant with the department, Joseph began research with the Mobile and Portable Radio Research Group (MPRG) at Virginia Tech. After continuing his GTA for an additional year of his research, he worked as a Graduate Research Assistant to MPRG under Dr. A. Annamalai, together having published two journal papers and one conference paper on Nakagami-m estimation techniques. Since February 2005, he has been continuing his research at Virginia Tech towards a Ph.D.